Canadian Science Publishing

ARTICLE

Multi-decadal shifts in the distribution and timing of Pacific herring (*Clupea pallasii*) spawning in Prince William Sound, Alaska

David W. McGowan, Trevor A. Branch, Stormy Haught, and Mark D. Scheuerell

Abstract: The location and timing of spawning play a critical role in pelagic fish survival during early life stages and can affect subsequent recruitment. Spawning patterns of Pacific herring (*Clupea pallasii*) were examined in Prince William Sound (1973–2019) where the population has failed to recover since its collapse in 1993. Abrupt shifts in spawn distribution preceded the rapid increase in population size in the 1980s and later its collapse by one and two years, respectively. Following the population collapse, spawning contracted away from historical regions towards southeastern areas of the Sound, and the proportion of occupied spawning areas declined from 65% to <9%. Spatial differences in spawn timing variation were also apparent, as the median spawn date shifted earlier by 26 days in eastern and 15 days in western areas of Prince William Sound between 1980 and 2006, and then shifted later by 25 (eastern) and 19 (western) days over a 7-year period. Effects of contracted spawning areas and timing shifts on first-year survival and recruitment are uncertain and require future investigation.

Résumé : Le lieu et le moment du frai jouent un rôle critique dans la survie des poissons pélagiques durant les premières étapes de la vie et peuvent avoir une incidence sur le recrutement subséquent. Nous avons examiné les motifs de frai du hareng du Pacifique (*Clupea pallasii*) dans le golfe du Prince William (1973–2019), où la population ne s'est pas encore rétablie dans la foulée de son effondrement en 1993. Des changements abrupts de la répartition du frai ont précédé, d'un et de deux ans respectivement, l'augmentation rapide de la population dans les années 1980 et son effondrement plus tard. Après l'effondrement de la population, l'aire de répartition du frai s'est contractée dans les secteurs historiques de frai pour se déplacer vers des secteurs du sud-est du golfe, et la proportion des lieux de frai occupés est passée de 65 % à <9 %. Des différences spatiales de la variation du moment du frai ressortent également, la date médiane du frai étant de 26 jours plus hâtive dans les secteurs est et de 15 jours plus hâtive dans les secteurs ouest du golfe en 2006 qu'en 1980, pour ensuite être repoussée de 25 jours (à l'est) et de 19 jours (à l'ouest) sur une période de 7 ans. Les effets de la contraction de la répartition du frai et des changements du moment du frai sur la survie et le recrutement durant la première année ne sont pas bien établis et nécessitent plus d'études. [Traduit par la Rédaction]

Introduction

The location and time of spawning plays a critical role in the survival of pelagic fish during early life stages that subsequently affects recruitment. For herring (*Clupea* spp.), spatial differences among spawning sites can influence embryo mortality rates (Rooper et al. 1999; Shelton et al. 2014; Keeling et al. 2017) and the transport and retention of larvae in nursery areas (Sinclair and Tremblay 1984; Cowan and Shaw 2002). Temporal shifts in spawning can affect the duration of egg and larval stages (Houde 2016), predation risk, and the availability of prey to larvae during the critical early feeding period (Cushing 1990).

A typical Pacific herring (*Clupea pallasii*, hereafter herring) population will collectively spawn batches of eggs over a period of days to months across numerous sites (Hay 1985), a strategy which is adapted to increase opportunities for herring offspring to survive early life stages. Although individual herring spawn once per season, staggered spawning across the entire population in space and time has the effect of hedging against uncertainty in the timing and location of optimal conditions for egg and larval survival (Lambert 1990). Spatial and temporal diversity in spawning among metapopulations also buffers the larger population from abundance fluctuations (i.e., the portfolio effect; Schindler et al. 2010) — herring spawning that is broadly distributed in space and time increases population resilience to perturbations in their environment (Hay 1985; Lambert 1987; Siple and Francis 2016). Accordingly, changes in the number or spatial diversity of spawning locations, and temporal shifts in the onset or duration of spawning may impact long-term productivity of herring populations (Ruzzante et al. 2006; Dragesund et al. 2008).

Spatial patterns of herring spawning are determined by population size and processes that affect fidelity to spawning areas and dispersal to new locations (Ware and Schweigert 2001; Flostrand et al. 2009). The persistence of spawning at known locations over a number of years indicates conservation of migration patterns across generations, while variations from established migration patterns indicates straying or diffusion that results in the

---

Received 2 March 2021. Accepted 4 April 2021.

D.W. McGowan* and T.A. Branch. School of Aquatic and Fishery Sciences, University of Washington, Box 355020, Seattle, WA 98195-5020, USA.
S. Haught. Division of Commercial Fisheries, Alaska Department of Fish and Game, P.O. Box 669, Cordova, AK 99574, USA.
M.D. Scheuerell. US Geological Survey, Washington Cooperative Fish and Wildlife Research Unit, School of Aquatic and Fishery Sciences, University of Washington, Box 355020, Seattle, WA 98195-5020, USA.

Corresponding author: David W. McGowan (email: david.mcgowan@noaa.gov).
*Present address: Alaska Fisheries Science Center, National Marine Fisheries Service, National Oceanic and Atmospheric Administration, 7600 Sand Point Way NE, Seattle, WA 98115, USA.

Can. J. Fish. Aquat. Sci. **78:** 1611–1627 (2021) dx.doi.org/10.1139/cjfas-2021-0047

colonization of new areas or reoccupation of previously active locations (Petitgas et al. 2006). Young herring are hypothesized to learn migration patterns by schooling with older, repeat spawners in the year before they first spawn and follow them to spawning areas, thereby increasing the likelihood of cross generation fidelity to the general spawning area in successive years (McQuinn 1997; Corten 2002; MacCall et al. 2019). If this hypothesis is true, variations in migration patterns would occur if the social learning process is disrupted due to naïve fish not mixing with older fish, stock collapse, or a predominance of naïve fish following a strong recruitment (Huse et al. 2002, 2010; Corten 2002). Unguided young herring may also be more likely to stray from migration patterns due to increased sensitivity to environmental conditions (Macdonald et al. 2018), thus expanding or shifting population distribution. Large perturbations in the environment may also affect adult migration patterns (Petitgas et al. 2006). Knowledge of spawning areas may be lost when a metapopulation experiences high mortality due to natural processes (e.g., disease outbreak, localized predation) or anthropogenic effects (fisheries, oil exposure), thereby affecting the diversity and number of spawning sites and potentially altering reproductive success.

In the Northeast Pacific, interannual variations in herring spawn timing have been primarily attributed to population demographics and temperature (Hay 1985; Ware and Tanasichuk 1989). Gonad maturation rate is determined by fish weight and daily temperature (Ware and Tanasichuk 1989), resulting in earlier spawning by larger fish and during warmer years. In populations comprising multiple age cohorts, spawning may be staggered in discrete waves with older fish spawning earlier than younger fish (Hay 1985; Ware and Tanasichuk 1989). If population age structure is dominated by one cohort or truncated by fishing (e.g., Barnett et al. 2017), spawning duration is likely to be shortened. State-dependent life-history modeling also suggests that variations in food availability to adult fish may result in spawn timing shifts to optimize self-fitness (Ljungström et al. 2019).

We examined changes in spawning patterns in a once-thriving herring population in Prince William Sound, Alaska. Herring are a key forage species in this ecosystem, and they have supported commercial fisheries for more than a century (Muradian et al. 2017). The population collapsed abruptly in 1993 (Quinn et al. 2001; Deriso et al. 2008; Hulson et al. 2008; Muradian et al. 2017) and has yet to recover to pre-collapse biomass levels due to a lack of strong year classes that recruit and carry through the adult population (Fig. 1A). There is uncertainty as to the causes of the initial population collapse and subsequent lack of recovery, with hypotheses including poor nutrition (Pearson et al. 1999, 2012), infectious disease (Rice and Carls 2007; Hulson et al. 2008), and the combined effects of the 1989 *Exxon Valdez* oil spill and overexploitation by the fishery (Thorne and Thomas 2008). Continued low population size and poor recruitment have been attributed to repeating disease cycles from multiple pathogens (Rice and Carls 2007), shifts in environmental conditions in the Gulf of Alaska (Pearson et al. 2012; Ward et al. 2017), humpback whale (*Megaptera novaeangliae*) predation (Pearson et al. 2012), competition with hatchery-released pink salmon (*Oncorhynchus gorbuscha*) (Deriso et al. 2008; Pearson et al. 2012), and cardiac abnormalities resulting from trace exposure to lingering oil (Incardona et al. 2015). Since the collapse, no recruitment events have come close to the magnitude of the 1980, 1981, 1984, and 1988 birth years (Muradian et al. 2017), and there have only been two cohorts of moderate size (1999, 2016 birth years) in the past 30 years (Fig. 1B; J. Trochta, University of Washington, personal communication, 23 December 2019), creating uncertainty as to which conditions are required for recovery.

The match–mismatch hypothesis (Cushing 1990) and portfolio effect (Schindler et al. 2010) highlight the critical influence that spawn timing and location, and diversity of spawning areas, have on herring reproductive success. We used a 47-year time series of spawning distributions in Prince William Sound from aerial survey data to examine (1) decadal and interannual shifts in the distribution of spawn locations; (2) interannual shifts in spawn timing; and (3) the spatial structure of spawning areas based on spawn timing trends. Recruitment dynamics and spatial patterns of population age structure, commercial harvest, and impacted coastline from the *Exxon Valdez* oil spill were also examined to assess whether shifts in spawning distributions coincided with spatial changes in recruitment and local exploitation, and the oil spill.

Fig. 1. Prince William Sound herring stock assessment model estimates for (A) median spawning stock biomass (SSB) and (B) number of age-3 recruits from 1980 to 2019 (J. Trochta, University of Washington, personal communication, 23 December 2019). Shaded area indicates 95% confidence interval. Cohort sizes greater than 220 million age-3 recruits (dashed line) are considered strong recruitment events (EVOSTC 2010).

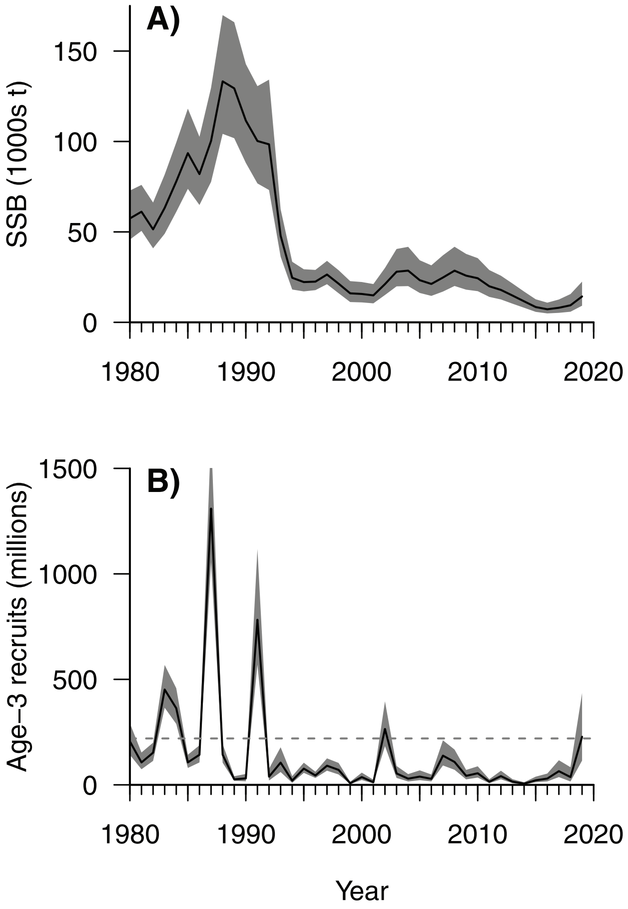

Materials and methods

Data collection

Active herring spawning was observed during aerial surveys conducted by the Alaska Department of Fish and Game (ADF&G) in the Prince William Sound management area between 1973 and 2019. The ADF&G aerial survey is a non-random survey that attempts to account for all spawning within the Sound. Weather, time, and funding constraints preclude implementation of a randomized or complete survey design; therefore, flight plans are based on the most recent information of where herring schools and spawning aggregations are most likely to be located from numerous sources

Fig. 2. Prince William Sound management area. Red box within the inset map of Northeast Pacific outlines the study area. Bathymetric (blue) and geographic (black) features mentioned in text are labeled. Maps created using ArcGIS 10.7.1 with data from the Alaska Department of Natural Resources (ADNR 2018) and Esri (Esri 2020). [Colour online.]

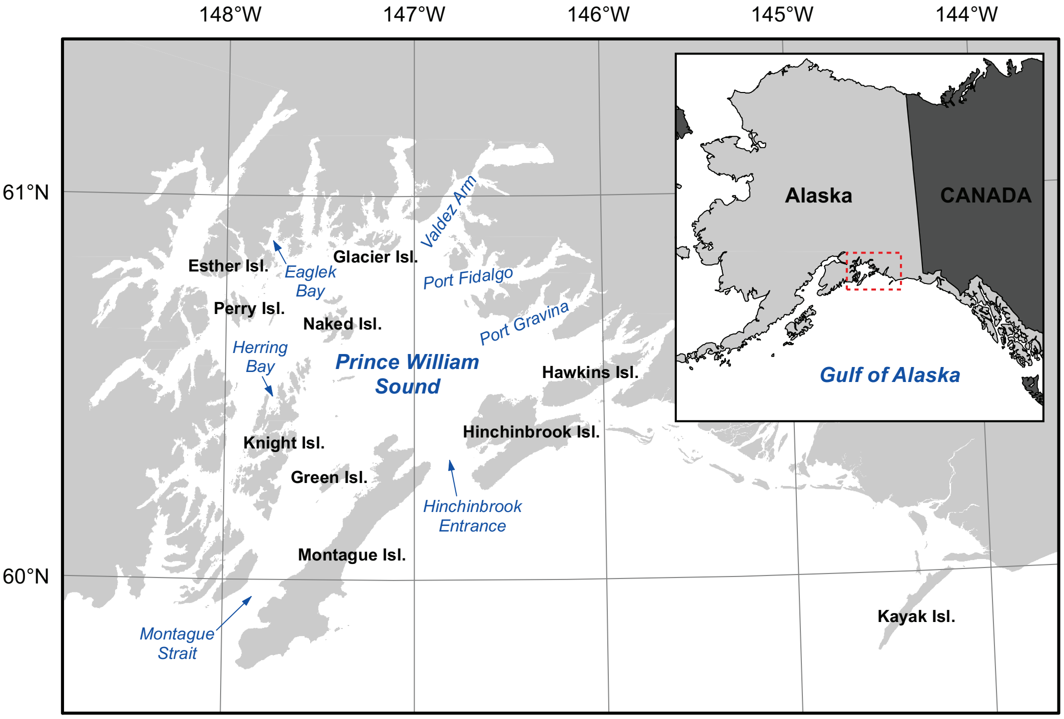

that include fish and marine mammal distributions from the prior day, reports from boats on the Sound, and observations from non-survey flight traffic.

Active herring spawn is measured as the total length of milt clouds along the coastline per day (mile-days of milt; 1 mile = 1.609 km) following Shepherd and Haught (2019). Mile-days of milt is a key index of relative abundance in the stock assessment for Prince William Sound herring (Muradian et al. 2017). Aerial surveys are flown between late-March and mid-May (refer to online Supplementary Table S1[1]). At the start of each spawning season, scheduled surveys are flown once or twice per week, and then flown more frequently (up to twice a day) when spawning or pre-spawning aggregations are observed. Surveys end when there is no observed spawning or anecdotal reports of spawning in the Sound. Surveys are flown along the coastline at approximately 460 m (1500 ft.) altitude for up to 5 hours, covering about 800 km (~500 mi) per survey.

Survey coverage has changed over the study period. Prior to 1981, coverage was primarily in the northern and eastern Sound from Glacier Island and lower Valdez Arm to Port Gravina, and the southern Sound along the northern coasts of Hawkins and Hinchinbrook islands and Northeast Montague Island (Fig. 2, Supplementary Fig. S1[1]). In the 1980s, surveys were expanded to the northern Sound west of Glacier Island to Esther Island, and in the western Sound to include Knight, Naked, and Perry islands. In 2007, additional surveys were flown infrequently over Kayak Island.

Prior to 2008, most surveys were conducted by a pilot and one observer who photographed and recorded spawn observations on paper maps (Brady 1987). Since 2008, an additional observer has been added and spawn observations are digitally recorded inflight as polylines using Esri ArcPad (Esri Inc., Redlands, California) with a Bluetooth GPS for georeferencing (Shepherd and Haught 2019). Post-processing of digital data uses photographs and video to refine the mile-days of milt data in ArcGIS (Esri Inc., Redlands, California). Observations originally recorded on paper maps were digitized as polylines in ArcGIS. Survey effort was converted to polygons from historical logbooks (1973 to 1999) or polylines for the later georeferenced flight paths (1997 to 2019). Processed spawn and survey effort data (1973 to 2018) are publicly available through the Alaska Ocean Observing System (https://portal.aoos.org, Bochenek 2010; Haught and Moffitt 2018), and were combined for this study with survey data from 2019.

Spatial analysis

Survey coverage and spawning data were partitioned into 10 km × 10 km grid cells (Fig. 3). ArcGIS polylines and polygons that occurred in two or more grid cells were split into segments at the borders of each cell. Polyline segments for mile-days of milt were assigned values equivalent to the length of the segment within the grid cell. Grid cells were assigned binary values for survey coverage (0 = no coverage, 1 = coverage) based on coverage polygon or polyline segments. Consistent with prior analyses of spawn patterns in Prince William Sound, grid cells were grouped into regions (Fig. 3) based on ADF&G herring districts within the Prince William Sound management area (e.g., Russell et al. 2017): Montague Island, Naked Island, North Shore, Northeast Shore, Southeast Shore, and Kayak Island.

Spatial patterns of herring spawning were characterized at decadal and interannual scales across Prince William Sound and by region from 1973 to 2019. To examine decadal spatial patterns, mile-days of milt (MDM) were summed within each grid cell by decade, and plotted by decade as quantiles of all years combined in 10% increments. To examine interannual spatial patterns, MDM values were summed within each grid cell by year from 1973 to 2019. Quantiles for annual MDM values were calculated in 20% increments for all years combined and plotted as heat maps

---

[1] Supplementary data are available with the article at https://doi.org/10.1139/cjfas-2021-0047.

Fig. 3. Boundaries for Prince William Sound regions and the Gulf of Alaska adapted from appendix G4 in Russell et al. (2017). Numbered 10 km × 10 km grid cells indicate areas within each region where herring spawning was observed between 1973 and 2019. Map created using ArcGIS 10.7.1 with data from the Alaska Department of Natural Resources (ADNR 2018).

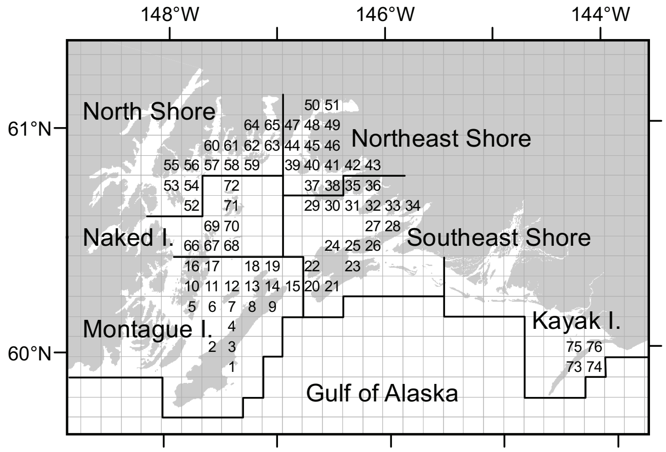

by year and grid cell. Grid cells with positive survey coverage values for each year were identified in the heat map to indicate interannual changes in the survey domain. To show interannual spatial variations in cumulative spawn, MDM values were summed across grid cells within each region by year.

To quantify interannual changes in how evenly distributed spawning was across Prince William Sound, we used an index of spatial dispersion (Payne et al. 2005) adapted from Pielou (1966) species evenness index, based in turn on Shannon's species diversity index (Shannon and Weaver 1949):

$$D_t = \frac{-\sum_{j=1}^{s} p_{j,t}\ln(p_{j,t})}{\ln(s)} \tag{1}$$

where $p_{j,t}$ is the proportion of total spawn (MDM) in each grid cell j in year t, and s is the total number of grid cells in which active spawning was observed within Prince William Sound in any year between 1980 and 2019. Observations from the 1970s and Kayak Island were not included in the dispersion index calculation due to gaps in survey coverage. Index values D_t range from 0 (all spawning in one grid cell) to 1 (evenly distributed across all grid cells). Although not all grid cells were surveyed each year, under this approach we assume that all grid cells were either directly sampled by the survey or indirectly via other methods (e.g., anecdotal reports from other aircraft or vessels) each year. It is not known what proportion of total spawn remains unobserved each year, but the dispersion index is assumed to be sufficiently robust to quantify relative changes in evenness given the high proportion of sites (>50%) that are sampled each year (Payne et al. 2005).

To assess if shifts in spawning distributions coincided with spatial changes in population age structure and recruitment patterns, age composition data were summarized within each region and compared to spawning spatial patterns. Herring age data have been collected from catches and surveys since the 1970s (Shepherd and Haught 2019), and are used in the stock assessment (Muradian et al. 2017). Age composition data were summarized for herring two years and older by region from 1980 to 2019 using commercial catch and survey samples collected by purse seine or cast net. Data were pooled for North Shore and Naked Island due to low sample sizes. We compared age compositions among the regions by year to determine if there were spatial differences in recruitment patterns of the seven largest cohorts with >220 million age-3 recruits (Fig. 1B; EVOSTC 2010; Muradian et al. 2017). We assessed whether regional differences in age structure coincided with changes in spawning distributions.

Commercial catch data were also summarized by region to assess whether local exploitation rates greater than 20% preceded sharp declines in spawning. This threshold was based on the maximum management target rate of 20% harvest for spawning biomass throughout Prince William Sound (Prince William Sound Herring Management Plan, 5 AAC 27.365(b)). Fish ticket records (ADF&G 2019*a*, 2019*b*) for the purse seine and gillnet sac-roe fisheries and the spawn-on-kelp pound fishery were summarized within each region from 1980 to 1999, the last year in which commercial fishing occurred. Landings from the sac-roe fisheries were reported in total whole fish weight (t). The pound fishery, in which herring were impounded to produce spawn-on-kelp, reported only the spawn-on-kelp product weight (t). To generate pound-fishery landings data equivalent to the sac-roe fisheries, we used a conversion factor developed by ADF&G to estimate the weight of utilized herring biomass, that assumes 12.5 t of herring would produce 1 t of spawn product (Morstad et al. 1992). For all fisheries, catch data were pooled for North Shore and Naked Island due to uncertainty in the location of some reported catches. The location of fishing associated with each fish ticket i was cross-referenced with sample locations from the age database and ADF&G annual management area reports to verify that commercial catches were accurately tallied within each region.

The exploitation rate (ER) of the commercial fishery in year t within each region n was calculated as

$$\mathrm{ER}_{n,t} = \frac{\sum_{i=1}^{f} h_{i,n,t}}{\frac{\mathrm{MDM}_{n,t}}{\mathrm{MDM}_t} \times \mathrm{SSB}_t} \tag{2}$$

(i.e., the sum of commercial landings from the three fisheries h divided by estimated spawning stock biomass (SSB) from the stock assessment). SSB was allocated to regions by assuming that MDM in each region is proportional to SSB in each region (see Fig. 3). A Pearson's χ^2 test for independence was used to determine if the probability of changes in spawning of ±50% from the prior year (ΔMDM) was similar under different levels of local exploitation. For each year and region, observations were categorized based on the change in total spawn from the prior year ($\Delta\mathrm{MDM} < -50\%$, $-50\% \leq \Delta\mathrm{MDM} \leq -50\%$, $\Delta\mathrm{MDM} > 50\%$) and whether the local exploitation rate from the prior year was either high ($\mathrm{ER} > 0.2$), low ($0 < \mathrm{ER} \leq 0.2$), or there was no fishing ($\mathrm{ER} = 0$). A separate 3 × 3 contingency table grouped observations based on exploitation in the prior two years: high ($\mathrm{ER} > 0.2$) in both years; no fishing ($\mathrm{ER} = 0$) in both years; or all other observations where exploitation was either high in only one year or low ($0 < \mathrm{ER} \leq 0.2$) in one or both years. P values were estimated using Monte Carlo simulations with 10 000 replicates.

Spawning patterns were also examined relative to the distribution of shoreline impacted by the *Exxon Valdez* oil spill. Spawn distributions were summarized into four periods: the decade prior to the spill (1980–1988); the year of the spill (1989); the three-year period following the spill that preceded the collapse of the herring population (1990–1992); and the post-collapse period (1993–2019). Shoreline oiling data are from surveys conducted in the summer and fall 1989 and spring 1990 that assessed coastline as being "very lightly" to "heavily" impacted by the spill and cleanup (ADNR 1996*a*, 1996*b*).

Temporal analysis

Interannual variation in spawn timing was examined across Prince William Sound and by region from 1980 to 2019, excluding

Table 1. Number of days of survey coverage (mean days·year^{-1}, $\bar{x}$, and standard deviation, SD) summarized by decade and region within Prince William Sound.

	All regions		Montague Island		Southeast Shore		Northeast Shore		North Shore		Naked Island		Kayak Island	
Decade	$\bar{x}$	SD	$\bar{x}$	SD	$\bar{x}$	SD	$\bar{x}$	SD	$\bar{x}$	SD	$\bar{x}$	SD	$\bar{x}$	SD
1970s	13.6	2.4	3.6	1.8	3.3	3.6	11.9	3.4	3.7	2.8	—	—	—	—
1980s	30.2	6.2	19.3	5.0	19.8	5.9	26.4	6.5	20.6	6.3	15.8	9.9	0.1	0.3
1990s	20.9	5.3	17.8	5.3	15.7	4.7	17.1	6.0	13.3	8.6	12.5	8.3	—	—
2000s	11.7	3.1	8.6	2.3	11.1	2.5	9.7	2.2	5.5	1.6	6.4	2.5	0.7	1.2
2010s	16.8	3.3	8.6	4.1	16.3	3.2	14.6	3.3	4.0	2.1	5.3	3.4	1.7	1.2

Note: A dash (—) indicates no survey coverage.

Table 2. Total spawn (mean mile-days of milt·year^{-1}, $\bar{x}$, and standard deviation, SD) summarized by decade and region within the Prince William Sound management area (note, the Kayak Island region is not shown due to inconsistent sampling).

	All regions		Montague Island		Southeast Shore		Northeast Shore		North Shore		Naked Island	
Decade	$\bar{x}$	SD	$\bar{x}$	SD	$\bar{x}$	SD	$\bar{x}$	SD	$\bar{x}$	SD	$\bar{x}$	SD
1970s	68.9	20.7	6.2	7.1	5.5	13.8	56.6	15.0	—	—	—	—
1980s	151.5	62.0	32.6	27.2	8.4	7.5	56.5	29.1	40.4	31.6	12.9	13
1990s	66.1	44.2	32.0	15.2	8.1	6.3	21.6	26.6	3.7	8.7	0.6	1.4
2000s	26.7	7.2	6.9	4.0	11.7	6.1	5.5	3.1	1.2	2.2	0.4	0.7
2010s	42.9	27.1	1.7	2.8	24.5	19.2	10.9	14.2	0.0	0.0	0.0	0.0

Note: A dash (—) indicates spatially limited or no survey coverage. 1 mile = 1.609 km.

observations from the 1970s and Kayak Island due to survey coverage gaps in space and time. MDM values were summed within each region by day of year (DOY) and year. Survey coverage and spawn events were plotted by DOY and year for each region and all regions combined. A time series of spawn timing was calculated for each region based on the day of year when 50% of total MDM for that year had been observed, which corresponds with the peak of spawning activity in most years (Supplementary Fig. S2[1]).

We fit multivariate autoregressive state-space (MARSS) models to time series of spawn timing for each region. The MARSS framework includes separate observation and process models to partition total variance between observation (i.e., sampling) and process (i.e., environmental perturbations) error (Holmes et al. 2012) and to estimate the underlying process that represents true spawn timing from multiple time series while accounting for missing values, autocorrelation among samples, and sampling error associated with aerial surveys. MARSS models can also be used to infer spatial structure of spawning areas to detect regional differences in spawn timing using Akaike's information criterion (AIC) model selection (e.g., Ward et al. 2010; Holmes et al. 2018*b*; Siple and Francis 2016).

The MARSS process model took one of two different matrix forms:

$$(3a)\qquad \boldsymbol{x}_t = \mathbf{B}\boldsymbol{x}_{t-1} + \boldsymbol{w}_t, \text{ where } \boldsymbol{w}_t \sim \mathrm{MVN}(0, \mathbf{Q})$$

$$(3b)\qquad \boldsymbol{x}_t = \boldsymbol{x}_{t-1} + \boldsymbol{u} + \boldsymbol{w}_t, \text{ where } \boldsymbol{w}_t \sim \mathrm{MVN}(0, \mathbf{Q})$$

Equation 3*a* is a mean-reverting stationary process, where the $m \times 1$ vector $\boldsymbol{x}_t$ represents true spawn timing for spawning area m in year t, $\mathbf{B}$ is an $m \times m$ matrix representing the strength of the autoregressive process for each state along the diagonal and zeroes elsewhere, and $\boldsymbol{w}_t$ is an $m \times 1$ vector of process errors drawn from a multivariate normal distribution (MVN) with mean vector $\boldsymbol{0}$ and variance-covariance matrix $\mathbf{Q}$. Equation 3*b* is a biased (non-stationary) random walk where $\boldsymbol{u}$ is an $m \times 1$ vector that represents an upward or downward bias in the random walk. We examined three process variance assumptions: (1) not correlated among the trajectories, with equal variances (same q value on the diagonal and zeroes elsewhere); (2) not correlated, with unequal variances (unique q_m values on the diagonal and zeroes elsewhere); or (3) correlated, with equal variances (same q value on the diagonal and the same g value elsewhere).

Our MARSS observation model was

$$(4)\qquad \boldsymbol{y}_t = \mathbf{Z}\boldsymbol{x}_t + \boldsymbol{v}_t, \text{ where } \boldsymbol{v}_t \sim \mathrm{MVN}(0, \mathbf{R})$$

where $\boldsymbol{y}_t$ is an $n \times 1$ vector of the observed spawn timing in region n in year t, $\mathbf{Z}$ is an $n \times m$ matrix containing 0s and 1s that maps each time series of observed spawn timing onto an associated true spawn timing $\boldsymbol{x}_t$ for each spawning area, and $\boldsymbol{v}_t$ is an $m \times 1$ vector of observation errors for each time series drawn from a multivariate normal distribution with mean vector $\boldsymbol{0}$ and variance-covariance matrix $\mathbf{R}$. Because the efficiency of aerial survey sampling may vary among regions, we assumed that sampling errors have unequal observation variances (i.e., unique r_n along the diagonal of $\mathbf{R}$) and are not correlated among time series (i.e., 0s in the off-diagonals of $\mathbf{R}$).

To assess spatial differences in spawn timing, we evaluated data support for 14 spawning area configurations among the five regions. Each model was modified to associate one or more of the observed time series with a corresponding process in $\boldsymbol{x}_t$. For example, when $m = 1$, data from all regions are treated as observations of a single spawning area; when $m = 5$, each region is modeled independently. For each of the configurations, we fit nine models in which the parameterization of $\mathbf{Q}$ was changed to test the three process error assumptions for three model structures: unbiased random walk (eq. 3*a*, $\mathbf{B}$ fixed at 1), biased random walk (eq. 3*b*), and stationary autoregressive process (eq. 3*a*, $\mathbf{B}$ estimated). Models were fit in R 3.4.3 (R Core Team 2020) using the "MARSS" package version 3.10.10 (Holmes et al. 2018*a*). Maximum likelihood estimates for parameters were obtained using the expectation-maximization algorithm (Holmes 2013).

We evaluated all 126 models for convergence and used residual scatterplots and autocorrelation function plots to verify that residuals were normally distributed and not autocorrelated in time. We assessed data support for each model using AIC for small sample size (AIC$_c$), with the most parsimonious models having the lowest AIC$_c$ value (Burnham and Anderson 2002).

Fig. 4. Distribution of spawning and extent of survey coverage from 1973 to 2019 by decade. Spawn patterns are represented as quantiles of mile-days of milt summed within each 10 km × 10 km grid cell by decade (plots A–E). Spawn patterns in the 1970s may be biased due to spatial and temporal gaps in coverage. Maps created using ArcGIS 10.7.1 with data from the Alaska Department of Natural Resources (ADNR 2018) and the Alaska Ocean Observing System (Bochenek 2010; Haught and Moffitt 2018). [Colour online.]

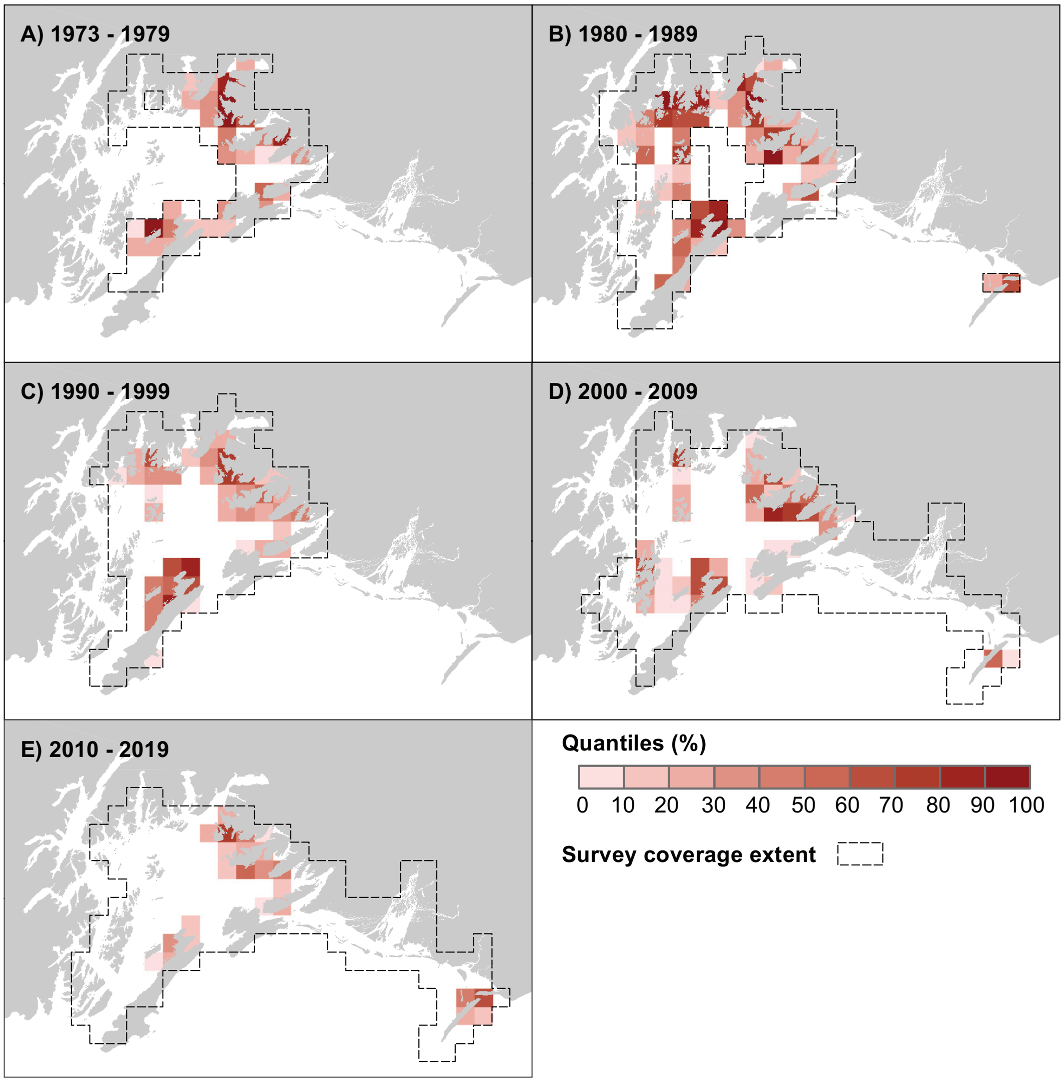

Models with $\Delta AIC_c < 2$ were considered statistically similar (Burnham and Anderson 2002).

Results

Spatial patterns

The ADF&G aerial survey coverage expanded and contracted over the 47-year study period. In the 1970s, survey coverage was primarily focused in the Northeast Shore region (11.6 days sampled per year versus <4 days·year^{-1} in other regions, Table 1). Coverage expanded across Prince William Sound in the early 1980s (Supplementary Table S1[1]), with flights occurring over all regions within the Sound on more than 50% of the days sampled per year (Table 1), peaking at 30 days·year^{-1} at the peak of population size (Fig. 1). Survey effort declined to 21 days·year^{-1} in the 1990s and 12 days·year^{-1} in the 2000s, reaching a low of 6 days sampled in 2004, and then increased to 17 days·year^{-1} in the 2010s. Survey coverage in the 1990s and 2000s remained above 40% of total days sampled for all regions within the Sound combined, except in 1995, 1996, 1999, and 2000 (Supplementary Table S1[1]). Kayak Island was not surveyed until 2007, except for one flight in 1982, and has since been sampled every year for 1 to 3 days, except in 2010 and 2016.

Pronounced decadal shifts occurred in the distribution of herring spawning within Prince William Sound. Spawning was primarily concentrated in the Northeast Shore and Montague Island regions in the 1970s — although this pattern may be biased due to unbalanced survey coverage — then expanded to all regions as the total cumulative spawn increased in the 1980s, before contracting towards Southeast Shore as spawning declined sharply in 1990s and remained low throughout the 2010s (Table 2; Fig. 4). Prior to the start of the population's rapid increase in biomass in 1983 (Fig. 1), spawning first expanded along North Shore and Naked Island during the early 1980s (Fig. 5), followed by increases in spawning along Montague Island and Northeast Shore a few years later as the population reached its peak size in 1988. Sharp declines in spawning along North Shore and Naked Island in 1990, and Northeast Shore in 1991, preceded the population's collapse in 1993 (Fig. 1). Following the collapse, spawning effectively ceased along North Shore and Naked Island, with only intermittent spawn events in the 1990s and 2000s, while

Fig. 5. Distribution of spawning from 1973 to 2019 by year. Spawn patterns are represented as (A) quantiles of mile-days of milt (MDM; 1 mile = 1.609 km) by 10 km × 10 km grid cell and year (note, quantiles were calculated across all years), and as (B) cumulative spawn within each region (MI = Montague Island; SE = Southeast Shore; NE = Northeast Shore; NS = North Shore; NI = Naked Island; KI = Kayak Island). Grid cell numbers (1–76) correspond to cell locations identified in Fig. 3. Gray dots indicate the extent of survey coverage (i.e., grid cells with no observed spawning). [Colour online.]

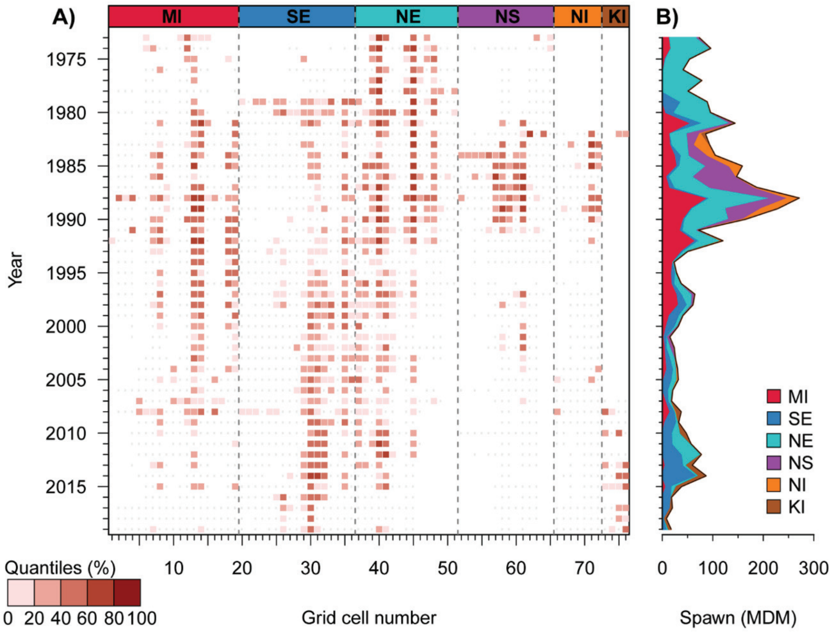

spawning remained low along Northeast Shore through 2010 as spawning within the region contracted southward. Following a brief increase in spawning during 2010–2012, activity along Northeast Shore declined to its lowest levels. Throughout the 1990s, Montague Island usually accounted for at least half of the total spawn, but spawning there steadily declined after 1999 (Fig. 5), and was not observed along Northeast Shore or Montague Island in 2016–2018. In contrast to the other regions within the Sound, spawning along Southeast Shore increased in the mid-1990s (Fig. 5B) and has accounted for the highest annual proportion of total spawn for the past two decades (Table 2).

Initially, herring consistently used at least half of the historical spawning areas throughout Prince William Sound until the 2010s, after which spawning distributions contracted to less than a third of the available areas as spawning biomass continued to decline to its lowest levels. Between 1980 and 2009, the dispersion index averaged 0.54 ± 0.07 (±1 standard deviation, SD), ranging from a peak of 0.65 in 1984 to a low of 0.35 in 1994, and did not differ between periods before and after the population collapse: 0.55 ± 0.06 in 1980–1993 versus 0.54 ± 0.06 in 1995–2009 (Fig. 6). Thus spatial increases in Southeast Shore spawning in the 1990s and 2000s offset declines in other regions (Figs. 4, 5). However, since 2010 dispersion declined sharply to 0.34 ± 0.13 as spawning contracted towards Southeast Shore, reaching an all-time low of 0.09 in 2018 (Fig. 6) that coincided with the most recent decline in spawning biomass (Fig. 1). Survey coverage in the 2010s (70% of all grid cells) was similar to that in 1995–2009 (72%) (Fig. 6). These results suggest that Prince William Sound herring now seldom use the primary spawning areas occupied in the 1980s, and active areas are currently concentrated along the Southeast Shore.

Spatial changes in spawning coincided with the appearance of large year classes. The rapid increase in population size during the 1980s (Fig. 1) was driven by the large 1976, 1980, 1981, and 1984 cohorts (Fig. 7). The total amount of spawn declined rapidly in the early 1990s as these year classes aged out of the population. Prior to their collapse, the 1988 cohort was the last strong year class to recruit to the spawning population.

Fig. 6. Spawning area dispersion index over time. Values of *D* range from 0 (highly aggregated) to 1 (evenly distributed). Survey coverage is represented by the proportion of grid cells sampled each year among the 72 cells in which spawning had occurred since 1980.

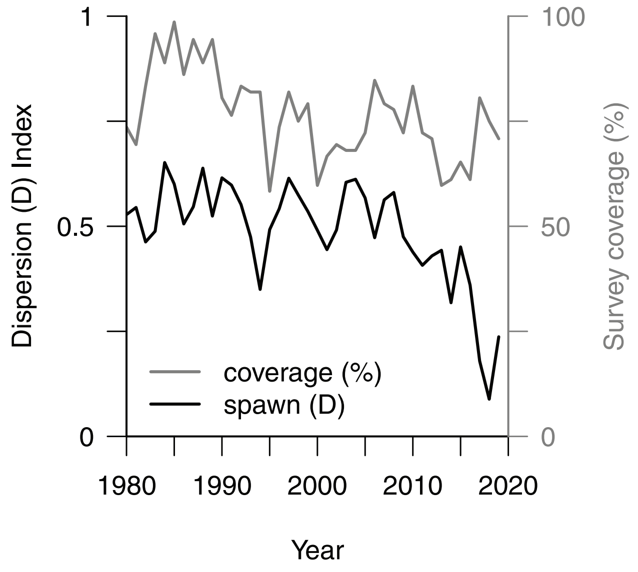

Unlike spatial patterns of spawning, there were minimal spatial differences in the age structure of herring in most years (Fig. 7). The seven largest cohorts typically accounted for a similar proportion of the age composition within each region. During the 40-year study period, regional differences in age structure were only apparent in six years (1987, 1991, 1994, 2001, 2007, and

Fig. 7. Herring age compositions by region and year from 1980 to 2019. Large cohorts (>200 million age-0 recruits) are highlighted in colour by birth year. The absence of a plot indicates no age data were collected from that region and year. [Colour online.]

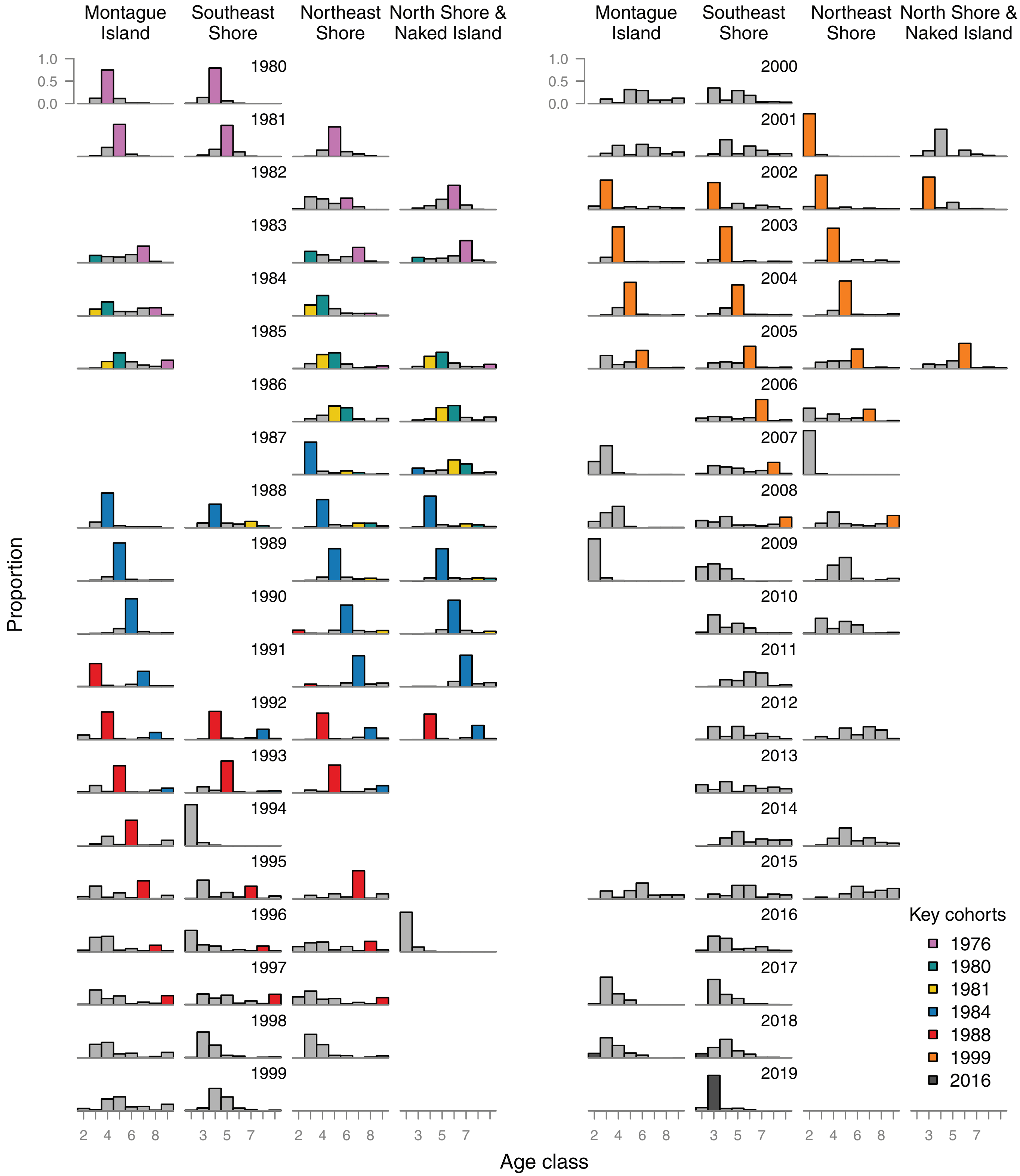

2008). Among these years, only in 1991 did spatial differences in age structure coincide with notable changes in spawning distributions. Age-3 fish from the 1988 cohort became the dominant year class for spawning aggregations in the Montague Island region in 1991 while the 1984 cohort remained the dominant year class in the North Shore, Naked Island, and Northeast Shore regions. This coincided with sharp declines in spawning from prior years in the northern regions, while total spawn

Fig. 8. Time series of (A) estimated herring spawning stock biomass (t) from 1980 to 2019 within each region (note, the North Shore and Naked Island regions are combined) showing the portion of the biomass estimate that was harvested by purse seine sac-roe, gillnet sac-roe, and pound spawn-on-kelp fisheries from 1980 to 1999. (B) Total survey-observed spawn (mile-days of milt; 1 mile = 1.609 km) and exploitation rate for all fisheries combined within each region (note, data are on separate axes). Harvest levels of less than 500 t are difficult to see in column A, but are included in exploitation rates shown in column B. [Colour online.]

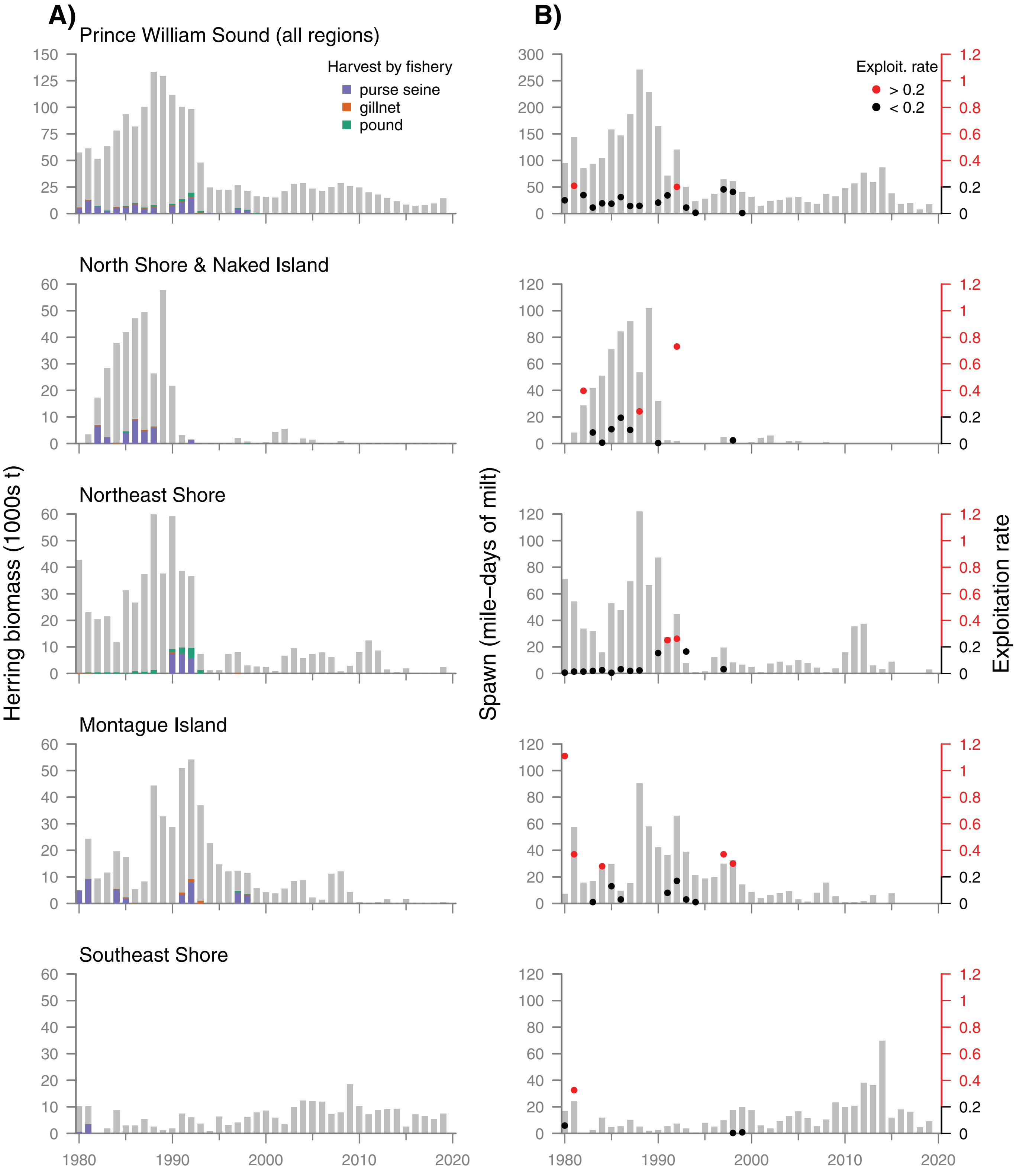

remained relatively stable along Montague Island but proportionally increased from a two-year average of 25% for all regions to 51% (Fig. 8). As the 1988 cohort established itself as the dominant year class across the Sound in the following years (Fig. 7), spawning effectively ceased along North Shore and Naked Island while briefly stabilizing along Northeast Shore before a two-decade period of low spawning activity (Fig. 8). In contrast, spawning along Montague Island fluctuated after the population collapse but remained the most active region through 1998, during which the 1988 cohort remained numerically dominant until 1996. With no strong year classes following the 1988 cohort (Fig. 1), spawning declined to consistently low levels along Montague Island by 2000 while spawning along Southeast Shore increased, largely due to the 1999 cohort.

It is unclear if shifts in spawning distributions followed changes in local exploitation by the fishery. In the 1980s, herring were primarily harvested along North Shore, Naked Island, and Montague Island. Overall exploitation rates for Prince William Sound remained below 0.2 in all years except 1981 (ER = 0.209) and 1992 (ER = 0.201) (Fig. 8), indicating that the intended harvest strategy was followed. While the population was spatially managed as a single stock throughout Prince William Sound, with total allowable catch allocated to multiple fisheries based on gear type and product, harvest was concentrated in only one or two regions each year. Local (region-specific) exploitation rates were greater than 0.2 in 3 of 7 years in North Shore–Naked Island, 2 of 3 years in Northeast Shore, 5 of 8 years in Montague Island, and 1 of 2 years in Southeast Shore (among regions where purse seiners harvested more than 500 t). The probability of changes in spawning was not significantly different under different levels of exploitation in the prior year ($\chi^2 = 6.81$, p value = 0.14; Supplementary Table S2[1]). However, decreases in spawning were more likely to occur following back-to-back years of local exploitation above 0.2 ($\chi^2 = 12.9$, p value = 0.0092; Supplementary Table S3[1]). This result is driven by three instances of back-to-back years with exploitation greater than 0.2 in the Northeast Shore (1991–1992) and Montague Island (1980–1981, 1997–1998) regions that preceded sharp declines in spawning the next year, all of which were followed by extended periods of relatively lower spawning within each region (Fig. 8).

Spawn patterns were not related to the distribution of shoreline impacted by the *Exxon Valdez* oil spill. Immediately following the spill, herring spawned in impacted areas along Naked Island and Montague Island (Supplementary Fig. S3[1]). Prior to the population collapse, sharp declines in spawning primarily occurred in regions that were not oiled (North Shore, Northeast Shore), while spawning fluctuated but remained relatively active near oiled areas along Montague Island throughout most of the 1990s (Figs. 5, 8). The exception was that spawning near oiled areas along Naked Island did decline sharply the year after the spill.

Temporal patterns

There was high interannual and regional variability in herring spawn timing from 1980 to 2019 (Fig. 9). The duration of the spawning season ranged from 4 days (2016) to 59 days (1986), being first observed on dates that spanned from 1 March in 2003 and 26 April in 1982, and last observed on dates ranging from 15 April (2005, 2011) to 21 May (1983, 2007). For all regions combined, the mean date of peak spawning (±1 SD, when 50% of cumulative total spawn was observed) was 17 April (DOY, 107 ± 7.5 days), and was earliest in Southeast Shore (12 April, 101.5 ± 9.1 days), and mostly progressed counter-clockwise from Northeast Shore (16 April, 106.3 ± 8.2 days), to North Shore (21 April, 110.9 ± 10.3 days), Naked Island (24 April, 113.8 ± 8.1 days), and Montague Island (23 April, 113.2 ± 7.7 days).

The two best MARSS models ($\mathbf{Z}_2$ and $\mathbf{Z}_{13}$; Table 3) reveal spatial differences in spawn timing. The $\mathbf{Z}_2$ model suggests separate spawn timing trajectories (i.e., $\boldsymbol{x}_t$) for the western Shore (Montague Island, Naked Island, and North Shore regions) and the eastern Shore (Southeast Shore, Northeast Shore regions), while the $\mathbf{Z}_{13}$ model further subdivided the eastern Shore trajectories by region (Table 3). Both models had correlated process errors with equal variances and estimated a stationary autoregressive process. Diagnostic plots found autocorrelated residuals for all MARSS models in which process errors were independent of other states (with either equal or unique variances) and were therefore rejected. $\mathrm{AIC_C}$ values for all random walk models ($\mathbf{B}$ fixed at 1) were consistently higher than corresponding models that estimated $\mathbf{B}$ (Table 3).

There is greater interannual variation in spawn timing along the western Shore ($\mathbf{Z}_2$:$b_{\boldsymbol{x}_1} = 0.25$; $\mathbf{Z}_{13}$:$b_{\boldsymbol{x}_1} = 0.27$) than the eastern Shore ($\mathbf{Z}_2$:$b_{\boldsymbol{x}_2} = 0.68$; $\mathbf{Z}_{13}$:$b_{\boldsymbol{x}_2} = 0.61$, $b_{\boldsymbol{x}_3} = 0.79$) (Table 4). These regional differences in spawn timing trajectories are most apparent between 1980 and 2006 when a shift to earlier spawning occurred at different rates along the eastern and western Shores (Fig. 10). During this 27-year period, spawn timing in the eastern Shore shifted earlier by 26 ($\mathbf{Z}_2$ model) to 30 days ($\mathbf{Z}_{13}$ model, Northeast Shore), while spawn timing was more variable in the western Shore and shifted earlier by 15 days in both models. Between 2006 and 2013, both models estimated that spawn timing shifted later by 23–26 days in the eastern Shore and 19 days in the western Shore, returning to the long-term mean spawn time in 2018 (Fig. 10).

The advantage of estimating separate spawn timing states for the eastern and western Shore is apparent when contrasted with the simplest model that estimated one state for all regions ($\mathbf{Z}_1$). The one-state model shows similar shifts in spawn timing in 2006 and 2013, but obscures east-west differences in the rate of change and interannual variability (Fig. 10) and had higher observation variances for all-time series than in the $\mathbf{Z}_2$ and $\mathbf{Z}_{13}$ models (Table 4).

Discussion

Spatial patterns

Herring no longer return to the historical spawning areas in Prince William Sound that were used during a three-decade period when the population reached its peak biomass over the past half century. Between 1973 and 1998, when the population increased from relatively low levels in the 1970s (Funk and Sandone 1990) to peak biomass in the late 1980s before collapsing in the early 1990s (Muradian et al. 2017), nearly all major spawning events occurred along Northeast Shore, North Shore, or Montague Island. After the collapse, contraction of spawning distributions and increased fidelity to general spawning areas would be expected due to relaxation of density-dependent processes as the population declines (Ware et al. 2000); yet spawning did not contract towards regions where spawning was historically high. Instead, spawning shifted towards Southeast Shore, where spawning was low prior to 1998, except briefly in 1979–1981. Despite substantial declines in total spawn, spatial diversity of spawning remained similar 15 years after the collapse compared to the precollapse period, as increased activity along Montague Island and later Southeast Shore largely offset decreased spawning in northern regions. This suggests that spatial diversity of spawning areas was not strongly related to spawning biomass at our analysis resolution (100 km^2), consistent with Hay et al.'s (2009) scale-dependent assessment of herring spawning patterns in British Columbia, until the population declined to historic lows (<10 t) in the 2010s. While decadal patterns of spawning depict this as a gradual change in distributions, abrupt shifts in interannual patterns during the early and late 1990s appear to be largely responsible for the long-term contraction to Southeast Shore.

These and other abrupt shifts in spawning distributions preceded major changes in population size. For example, spawning first expanded into western areas of North Shore and Naked

Fig. 9. Distribution of spawn timing (day-of-year, DOY) from 1980 to 2019 by (A–E) region and (F) for all regions within Prince William Sound (PWS) combined. Daily spawn total is scaled by total mile-days of milt (1 mile = 1.609 km) observed within each region. Each plot shows a time series of the median spawn date, and the mean spawn dates across all years. Survey coverage indicates days in which no spawning was observed within the region during the survey. [Colour online.]

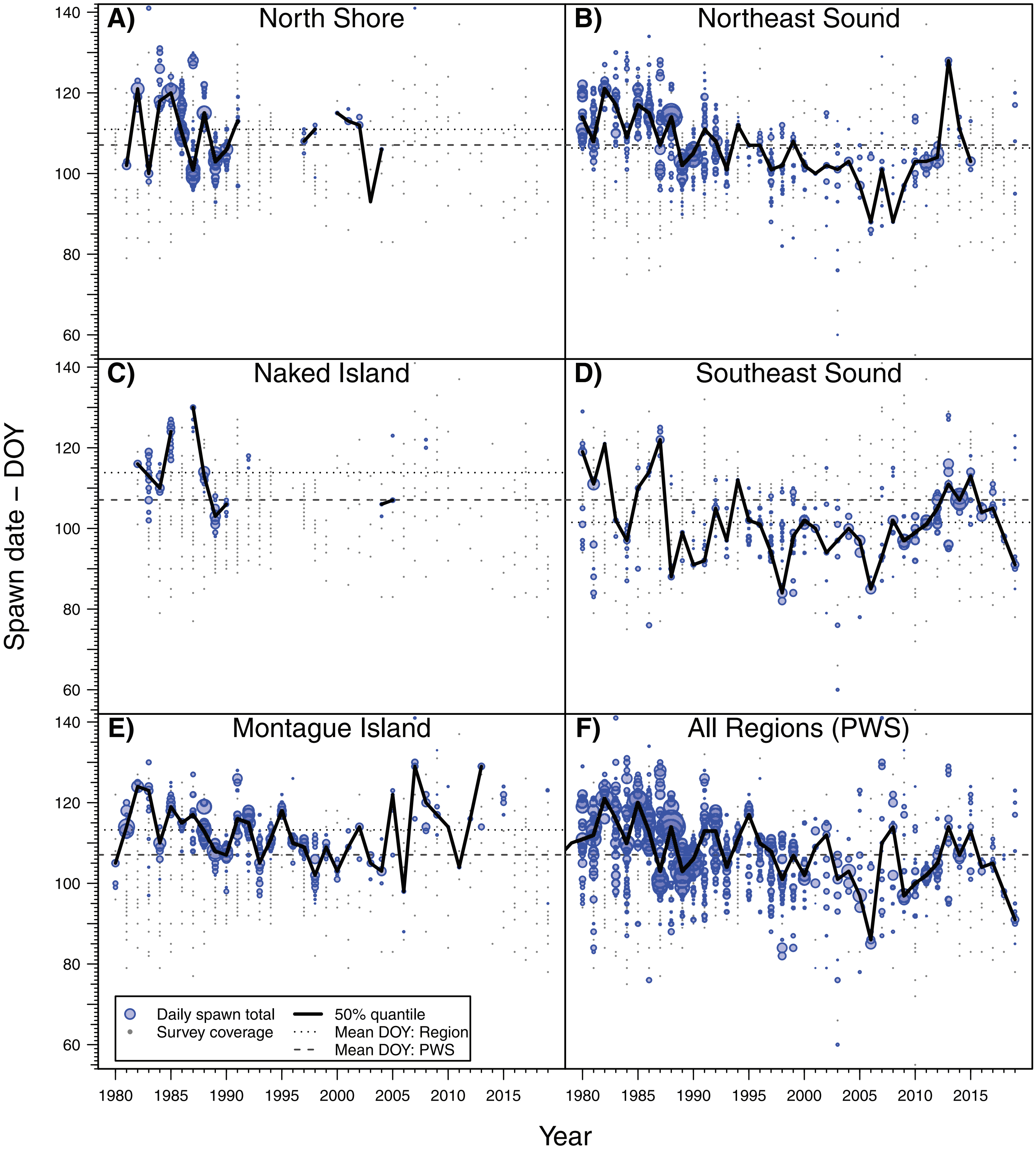

Island the year before the rapid increase in population size began in 1983. Similarly, sharp declines in spawning along North Shore and Northeast Shore occurred two years before the 1993 population collapse and again before more recent abundance declines in the late 1990s and early 2010s along Montague Island. It is possible that these shifts in spawning distributions resulted from increased straying among regions. There is high spatial variability in the rate of fidelity to spawning locations in British Columbia

Table 3. Model performance based on Akaike's information criterion corrected for small sample size (AIC_c).

						$\mathbf{Q}$ = equal variance and covariance					
	Spawning area state(s) ($\boldsymbol{x}_m$)					$\mathbf{B}$ = 1				$\mathbf{B}$ = unique	
	W. PWS			E. PWS		$\boldsymbol{u}$ = zero		$\boldsymbol{u}$ = unique		$\boldsymbol{u}$ = zero	
Num	MI	NS	NI	SE	NE	$\Delta\text{AIC}_\text{cc}$	k	$\Delta\text{AIC}_\text{c}$	k	$\Delta\text{AIC}_\text{c}$	k
$\mathbf{Z}_1$	1	1	1	1	1	15.0	7	17.3	8	**11.2**	8
$\mathbf{Z}_2$	1	1	1	2	2	10.6	9	9.1	11	**0.0**	11
$\mathbf{Z}_3$	1	2	1	2	2	16.2	9	14.6	11	8.2	11
$\mathbf{Z}_4$	1	2	2	1	1	18.5	9	17.7	11	11.6	11
$\mathbf{Z}_5$	1	2	2	1	2	19.7	9	24.0	11	17.3	11
$\mathbf{Z}_6$	1	2	1	1	2	19.7	9	22.9	11	15.3	11
$\mathbf{Z}_7$	1	2	2	2	2	18.3	9	17.4	11	10.1	11
$\mathbf{Z}_8$	1	1	1	2	1	19.7	9	20.6	11	9.6	11
$\mathbf{Z}_9$	1	1	1	1	2	17.9	9	20.0	11	9.3	11
$\mathbf{Z}_{10}$	1	2	1	3	2	21.2	10	19.3	13	9.9	13
$\mathbf{Z}_{11}$	1	2	2	1	3	21.6	10	20.3	13	10.0	13
$\mathbf{Z}_{12}$	1	2	2	3	2	22.3	10	21.5	13	—	13
$\mathbf{Z}_{13}$	1	1	1	2	3	16.4	10	14.0	13	**0.9**	13
$\mathbf{Z}_{14}$	1	2	3	4	5	25.4	12	20.5	17	7.0	17

Note: The **Z** matrix for each spawning area configuration (numbered $\mathbf{Z}_1$ to $\mathbf{Z}_{14}$) indicates corresponding states ($\boldsymbol{x}_{1\text{–}5}$) among the region time series in western or eastern Prince William Sound (W. PWS, E. PWS): MI = Montague Island; NS = North Shore; NI = Naked Island; SE = Southeast Shore; NE = Northeast Shore. Results for three model structures are shown for each Z matrix, including $\Delta\text{AIC}_\text{c}$ values that are relative to the best model (AIC_c), and the number of parameters (k). Process errors (**Q**) were estimated with equal variances that were correlated (equal variance and covariance). The diagonal of the **B** matrix was set to 1 (i.e., random walk) or estimated for each state (unique). Bias ($\boldsymbol{u}$) was either set to zero or estimated for each of the random walk models (unique). Bold $\Delta\text{AIC}_\text{c}$ values indicate the three models shown in Fig. 10. A dash (—) indicates a model that did not converge.

Table 4. Parameter estimates (Est) and standard errors (SE) for models in bold in Table 3 identified by their respective Z matrix configuration.

	Model form					
	$\mathbf{Z}_1$		$\mathbf{Z}_2$		$\mathbf{Z}_{13}$	
Coefficient	Est	SE	Est	SE	Est	SE
Observation variance (**R**)						
r_MI	41.72	11.71	28.53	10.12	31.97	10.03
r_SE	45.79	12.26	41.55	11.68	38.31	11.9
r_NE	36.58	10.49	27.02	8.81	25.51	9.14
r_NS	111.36	38.21	79.75	28.42	84.02	29.39
r_NI	32.82	16.13	29.55	15.46	30.05	15.14
AR strength (**B**)						
$b_{\boldsymbol{x}_1}$	0.59	0.19	0.25	0.24	0.27	0.25
$b_{\boldsymbol{x}_2}$			0.68	0.12	0.61	0.13
$b_{\boldsymbol{x}_3}$					0.79	0.09
Process variance–covariance (**Q**)						
q_diag	15.36	7.08	20.88	7.7	18.51	7.38
c_offdiag			17.99	7.08	17.51	6.5
Estimated state value $\boldsymbol{x}_t$ at time 0						
$\mu_{\boldsymbol{x}_1}$	9.79	9.5	–31.53	42.25	–30.25	40.17
$\mu_{\boldsymbol{x}_2}$			16.59	9.45	28.57	14.13
$\mu_{\boldsymbol{x}_3}$					9.28	7.65

herring within a comparable spatial resolution (statistical areas, ~500–2500 km^2) to regions within Prince William Sound (~700–1900 km^2), and that on average 40% of herring stray to spawn locations in other statistical areas the following year (Hay et al. 2001). Nonetheless, the persistence of spawning within each region in Prince William Sound for periods of a decade or longer, regional differences in spawn timing, and evidence of weak genetic differentiation between herring in the eastern and western Sound (Wildes et al. 2018) suggests that abrupt shifts in spawning within Prince William Sound did not result from random straying.

The occurrence of abrupt shifts in spawning one to two years prior to changes in population size suggests other factors have greater influence on fidelity to general spawning areas in Prince William Sound than spawning biomass. While it is beyond the scope of this study to quantify mechanistic relationships between spawning distributions and explanatory factors, we briefly explore how abrupt shifts in spawning are related to different intrinsic and extrinsic factors to identify potential mechanisms for future studies to investigate. These include: spatial variation in recruitment, effects of social and environmental cues on migration behavior, the 1989 *Exxon Valdez* oil spill, and increased local mortality related to disease, fishing, and predation.

Potential mechanisms for spatial shifts in spawning

Recruitment

One of the abrupt shifts in spawning distributions coincided with spatial variations in recruitment. In the 1980s, recruits from the three strong cohorts (1980, 1981, and 1984) that were responsible for driving biomass to record highs (Fig. 1) were widely distributed among spawning areas in most regions (Fig. 7), and large spawn events occurred annually in at least three regions (Figs. 5, 8). In contrast, recruits from the last strong cohort (1988) primarily spawned along Montague Island in 1991 as age-3 fish and not in the northern regions where spawning had declined sharply that year or the previous year. Spawning was not observed along North Shore over the next five years, but increased along Montague Island and Northeast Shore where the 1988 cohort became the dominant age class in 1992 as age-4 fish. Regional differences in age structure were not evident during the other major shift in spawning distributions towards Southeast Shore in the late 1990s, nor when recruits from the 1999 and 2016 cohorts first spawned.

Migration behavior

Herring migration behavior is influenced by social and environmental cues (Corten 2002), but the relative importance of

Fig. 10. Estimated time series of spawn timing ($\boldsymbol{x}_m$, solid line) based on MARSS models in bold in Table 3 (shaded area indicates the 95% confidence interval). Time series are centered by their mean for all years (dashed line) to indicate earlier (–) and later (+) median spawn date. Results for each model are shown by column (labels indicate the model's respective **Z** matrix). Rows within columns indicate the different regional groupings with unique spawning area configurations that correspond with shaded areas in map (top row). Maps created using ArcGIS 10.7.1 with data from the Alaska Department of Natural Resources (ADNR 2018). [Colour online.]

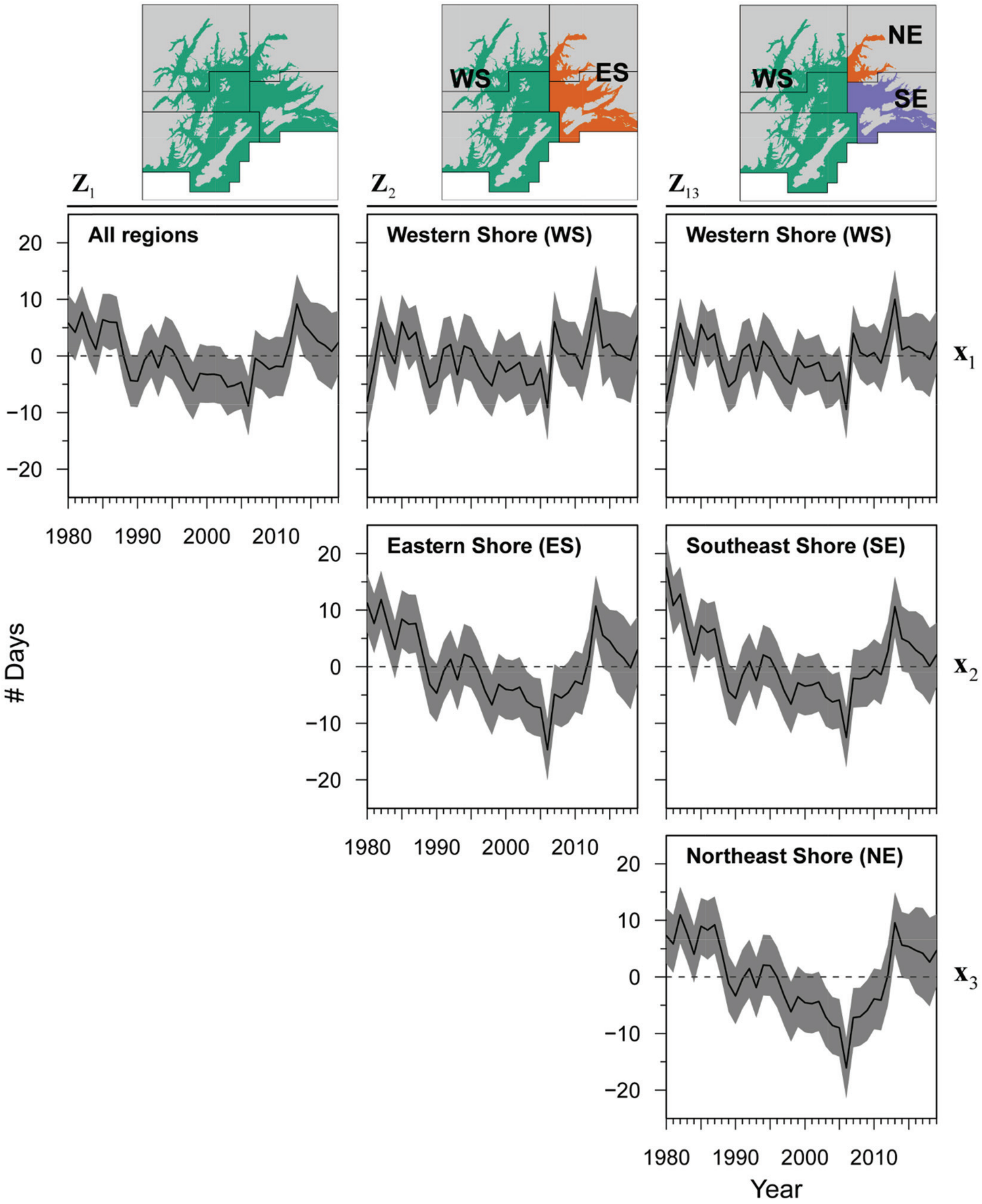

such cues is unknown for the Prince William Sound population. Spatial differences in herring recruitment between the 1980s and early 1990s is potentially related to social behavior and availability of older herring with knowledge of migration routes to spawning areas. Herring that spawn for the first time are hypothesized to school with and follow older, experienced fish and spawn in the same locations (McQuinn 1997; Corten 2002; MacCall et al. 2019). Abrupt declines in spawning biomass that coincide with an influx of numerically dominant recruits will reduce spatial overlap between age classes prior to spawning and disrupt the learning process necessary for first-time spawners to return to a general spawning area in successive years (Huse et al. 2002, 2010; Corten 2002). Likewise, the extent of spawning distributions in one year will likely influence spatial variation in recruitment the next year. If first-time spawners are guided by social cues, age composition data would be similar across regions where spawning was active the prior year. In contrast, abrupt shifts in spawning prior to a large influx of recruits that coincides with regional differences in age structure (e.g., 1991) would suggest changes in spawning distributions influenced migration paths of first-time spawners that led to spatial differences in recruitment.

Environmentally driven changes in migration patterns may also have influenced shifts in spawning distributions. A long-term warming trend in Prince William Sound has resulted in spatially complex changes in hydrographic conditions that are most pronounced in the northwest part of the Sound where the effect of glacial meltwater is highest (Campbell 2018). Spawning declines were first evident in northern regions, which have rarely been used by the population since the early 1990s. Changes in hydrographic conditions at spawning locations or along migration paths, including deepening of the seasonal mixed layer, cooling and freshening of surface waters via increased freshwater inputs from melting ice, and warming and increasing salinity of waters at depth (Campbell 2018), could potentially have increased straying to other areas if the population is adapted to select spawning habitat within narrow ranges of temperature and salinity (e.g., Haegele and Schweigert 1985).

Oil spill

It might be expected that herring would avoid spawning near shoreline impacted by the oil spill (Thorne and Thomas 2008). However, as also found by Pearson et al. (2012), sharp declines in spawning after the oil spill occurred primarily in northern regions that were not impacted by oil and cleanup efforts, while immediately after the oil spill, herring spawned within regions directly impacted by the spill and continued to spawn near impacted shoreline along Montague Island (Supplementary Fig. S3[1]). Spawning near oiled areas along Naked Island did decline sharply the year after the spill, but this region contributed relatively little to total spawn prior to the collapse (Fig. 5).

Increased local mortality

Spawning shifts may have also resulted from spatial changes in mortality rates for adult herring linked to disease outbreaks, fishing, and predation. Population-level effects of outbreaks of the protozoan parasite *Ichthyophonus hoferi* and the North American strain of viral hemorrhagic septicemia virus (VHSV) in Prince William Sound have garnered considerable attention since the 1990s, given that high disease-related mortality among adult herring in winter 1992–1993 is hypothesized to be a primary (Rice and Carls 2007; Hulson et al. 2008) or contributing (Deriso et al. 2008; Pearson et al. 2012) factor responsible for the population collapse in 1993, and that recurring outbreaks from multiple pathogens along with poor recruitment are inhibiting population recovery (Rice and Carls 2007; Marty et al. 2010). Despite increasing population-level mortality rates, disease outbreaks have not consistently coincided with declines in total spawn or contracted distributions. Among four disease outbreaks that occurred between 1994 and 2005 (Marty et al. 2010), only the 1998 outbreak coincided with notable shifts in spawning distributions: spawning declined sharply along Northeast Shore in 1998 and Montague Island in 1999, while remaining stable along Southeast Shore until 2001. Increased VHSV prevalence among herring (particularly younger fish) and concentrations of VHSV in water samples were correlated with confinement in closed spawn-on-kelp pounds during the 1998 outbreak (Hershberger et al. 1999), but the study pounds were located in the Southeast region where spawning remained stable for the next several years. It remains unknown if pound fishery operations amplify disease outbreaks among wild herring to effect mortality rates at the region or population level. Localized increases in mortality from disease outbreaks are plausible, particularly if the impacts of a pathogen are age-specific (e.g., Marty et al. 2010). However, we found no evidence of regional differences in age structure during this period (Fig. 7) as would be expected from a local outbreak, and examination of regional differences in disease prevalence was not possible in most years due to data limitations (Rice and Carls 2007).

Changes in predation may also have resulted in increased herring mortality at regional or finer spatial scales, but data were insufficient to examine this relationship. In fall and winter, predation by the increasing humpback whale population is a major source of mortality for overwintering and pre-spawning herring (Pearson et al. 2012; Moran et al. 2018), while adult and juvenile herring are important prey for pinnipeds (Rice et al. 2011), seabirds (Bishop et al. 2015), and groundfish (Gray et al. 2019) in winter. It is unclear how predation on pre-spawning aggregations influenced historical spawning patterns, either by disrupting herring migrations to spawning areas or reduce spawning aggregations, due to data limitations prior to 2008.

In contrast, availability of spatially indexed fishery catch data facilitated assessing whether shifts in spawning were related to local exploitation by fisheries. Annual sound-wide exploitation at the population level was at or below the management target rate of 0.2 in all years, and we found that regional declines in spawning were not related to local exploitation in the prior year (Supplementary Table S2[1]). This is consistent with Hay et al.'s (2008) comprehensive analysis of herring roe fisheries in British Columbia that did not find clear evidence that decreases in spawning frequency or declines in the number of spawning locations were related to fishing. Decreases in spawning within a region were significantly more likely to occur following back-to-back years of local exploitation above 0.2 (Supplementary Table S3[1]), although this is based on only three observations. In British Columbia, high local exploitation contributed to the depletion of herring subpopulations prior to an overall population decline (Okamoto et al. 2020).

Temporal patterns

Trends in spawn timing were also apparent over decadal and interannual scales, along with spatial differences in the magnitude of temporal variation between the eastern and western Sound. During the study period, spawning shifted earlier by 2–4 weeks over two decades, then reverted to later in the season by 3–4 weeks over the next six years, and finally shifted back to earlier dates over the next five years. Spawning patterns for the Sitka Sound herring population in coastal Southeast Alaska (c.f. figure 2 in Hebert 2019) provide context to temporal variation in Prince William Sound spawning. The occurrence of spawn timing shifts in Sitka (1998–1999, 2011–2012, and 2016–2017) do not coincide with major shifts in Prince William Sound (2006–2007, 2013–2014), indicating spawn timing is likely influenced by local factors such as temperature and population demographics (Hay 1985; Ware and Tanasichuk 1989). The magnitude of temporal variation is similar among the populations, suggesting spawn timing may be bounded by processes operating across the Gulf of Alaska that have lagged effects on local conditions near spawning areas.

While the mechanism for the multi-decadal trend towards earlier spawning is unknown, temporal shifts in 2006–2007 and 2013–2014 coincided with transitions between multi-year periods of ocean temperature anomalies in Prince William Sound and the Gulf of Alaska (figure 14 in Campbell 2018). Warm conditions persisted from 2001–2006, cold conditions from 2007–2013, and the Northeast Pacific marine heatwave occurred from 2014–2016 (Bond et al. 2015; Di Lorenzo and Mantua 2016). The coincidence of observed shifts in spawn timing with transitions between warm and cold periods is consistent with expected effects that temperature has on herring gonad maturation rates (Hay 1985; Ware and Tanasichuk 1989).

Demographic changes may also contribute to abrupt shifts in spawn timing trends, similar to how spatial variations in age structure coincided with shifts in spawning distributions in the early 1990s. Age-related differences in spawn timing are well documented from long-term observations for herring populations in British Columbia (Hay 1985) and the Atlantic (Lambert 1987). Similar effects of temperature and demography on spawn timing have been shown for other species, such as walleye pollock (*Gadus chalcogrammus*) in the Gulf of Alaska (Rogers and Dougherty 2019) and capelin (*Mallotus villosus*) in the Northwest Atlantic (Carscadden et al. 1997).

Potential consequences of spawning shifts

Spatial shifts in herring spawning may have contributed to the Prince William Sound population collapse. There is general consensus that high natural mortality in 1992–1993 resulted in the population collapse (Quinn et al. 2001; Deriso et al. 2008; Hulson et al. 2008; Muradian et al. 2017), although an alternate hypothesis suggests a major decline started earlier in 1989 due to the oil spill (Thorne and Thomas 2008). Although the mechanism for the high mortality remains uncertain, poor condition of herring prior to the collapse — likely due to poor nutrition resulting from environmentally driven low prey supply while biomass levels remained high (Pearson et al. 1999, 2012) — may have increased their susceptibility to multiple pathogens that triggered an outbreak (Rice and Carls 2007; Hulson et al. 2008). Rice and Carls (2007) hypothesized that declines in spawning starting in 1990 — due to the sharp decline along the North Shore and Naked Island (Figs. 5, 8) — concentrated spawning aggregations while biomass levels remained high, and that increases in crowding among spawning aggregations while in poor condition may have increased disease transmission (Marty et al. 2003).

The combined effects of low total spawn, reduced diversity of spawning areas, and concentration of spawning along the Southeast Shore may also be inhibiting first-year survival and contributing to the persistence of poor recruitment. Declines in total spawn and spatial diversity of spawning areas have impacted the population's spawning portfolio (i.e., the spatial and temporal diversity of spawning, Schindler et al. 2010), reducing opportunities for offspring to be dispersed to nursery areas that facilitate high first-year survival (Norcross and Brown 2001; Pineda et al. 2007; Rice and Carls 2007). The impacts of a reduced spawning portfolio may be amplified by the contraction of spawning to the Southeast Shore region rather than to other historical spawning areas. Herring larvae spawned along the Southeast Shore are more frequently retained in local nursery areas compared to larvae spawned in other regions that are widely dispersed to all areas of the Sound (Norcross and Brown 2001; Pegau 2013). Limiting larval dispersal to a fraction of available nursery areas reduces the likelihood that offspring are retained in nursery habitat whose suitability may vary from year-to-year. Prey quality and survival rates of juvenile herring during their first winter are also relatively lower in the Southeast Shore region compared to the other regions (Norcross and Brown 2001; Gorman et al. 2018).

Reproductive timing also plays an important role in determining recruitment success by influencing the coincidence of larvae with prey during critical periods (Cushing 1990), but it is uncertain whether shifts in spawn timing are linked to first-year herring survival in Prince William Sound. Variation in spawn timing may compensate for reduced spatial elements of the spawning portfolio, but these dynamics are poorly understood for this herring population. Future work is needed to quantify connectivity between known spawn locations and nursery areas under different oceanographic conditions throughout the spawning season, and to examine how temporal shifts in spawning correspond with variations in timing, magnitude, and duration of the spring bloom that affect prey quality and availability to larval herring. An improved understanding of how spatiotemporal variation in spawning and correspondence with secondary production influences larval dispersal and first-year survival would facilitate incorporating the effects of spawning dynamics on recruitment estimates.

Acknowledgements

This study was possible due to dedicated efforts of the pilots and observers that have conducted the ADF&G aerial survey since 1973, and those who digitized survey data from historical maps. We thank ADF&G staff M. Foster, K. Hebert, S. Moffitt, and T. Otis, along with T. Francis, S. Pegau, O. Shelton, E. Ward, and members of the Herring Research and Monitoring program for their insightful conversations on herring that improved the study design. Special thanks to A. MacCall for inspiring our research questions, and J. Trochta for sharing outputs from the stock assessment. Comments from S. Dressel, O. Ormseth, L. Rogers, C. Siddon, B. Templin, members of the *Exxon Valdez* Oil Spill Trustee Council (EVOSTC) Science Panel, and two anonymous reviewers improved earlier versions of the manuscript. This project was funded by the EVOSTC, and T.A.B. was funded in part by the Richard C. and Lois M. Worthington Endowed Professor in Fisheries Management. Findings and conclusions presented by the authors do not necessarily represent views of EVOSTC, NOAA, or ADF&G. Any use of trade, firm, or product names is for descriptive purposes only and does not imply endorsement by the US Government or State of Alaska.

References

ADF&G. 2019*a*. Statewide electronic herring fish ticket database 1985 to present. 1st ed. [accessed 17 September 2019].

ADF&G. 2019*b*. Statewide electronic herring fish ticket database 1969 to 1984. 1st ed. [accessed 17 September 2019].

ADNR. 1996*a*. *Exxon Valdez* Oil Spill - shoreline oiling - PWS summer 89. Available from http://asgdc.alaska.gov#1332 [accessed 24 June 2020].

ADNR. 1996*b*. *Exxon Valdez* Oil Spill - shoreline oiling - PWS fall/89 - spring/90. Available from http://asgdc.alaska.gov#1281 [accessed 24 June 2020].

ADNR. 2018. Alaska excluding small islands 1:63,360. Available from https://gis.data.alaska.gov/.

Barnett, L.A.K., Branch, T.A., Ranasinghe, R.A., and Essington, T.E. 2017. Old-growth fishes become scarce under fishing. Curr. Biol. **27**(18): 2843–2848.e2. doi:10.1016/j.cub.2017.07.069. PMID:28918949.

Bishop, M.A., Watson, J.T., Kuletz, K., and Morgan, T. 2015. Pacific herring (*Clupea pallasii*) consumption by marine birds during winter in Prince William Sound, Alaska. Fish. Oceanogr. **24**(1): 1–13. doi:10.1111/fog.12073.

Bochenek, R.J. 2010. PWS herring data portal. EVOS Restoration Project Final Report. Axiom Consulting & Design, Anchorage, Alaska.

Bond, N.A., Cronin, M.F., Freeland, H., and Mantua, N. 2015. Causes and impacts of the 2014 warm anomaly in the NE Pacific. Geophys. Res. Lett. **42**(9): 3414–3420. doi:10.1002/2015GL063306.

Brady, J.A. 1987. Distribution, timing and relative biomass indices for Pacific herring as determined by aerial surveys in Prince William Sound 1978 to 1987. ADF&G, Prince William Sound Data Report No. 87-14, Cordova, Alaska.

Burnham, K.P., and Anderson, D.R. 2002. Model selection and multimodel inference: a practical information-theoretic approach. 2nd ed. Springer, New York.

Campbell, R.W. 2018. Hydrographic trends in Prince William Sound, Alaska, 1960–2016. Deep-Sea Res. Part II Top. Stud. Oceanogr. **147**: 43–57. doi:10.1016/j.dsr2.2017.08.014.

Carscadden, J., Nakashima, B.S., and Frank, K.T. 1997. Effects of fish length and temperature on the timing of peak spawning in capelin (*Mallotus villosus*). Can. J. Fish. Aquat. Sci. **54**(4): 781–787. doi:10.1139/f96-331.

Corten, A. 2002. The role of "conservatism" in herring migrations. Rev. Fish Biol. Fish. **11**(4): 339–361. doi:10.1023/A:1021347630813.

Cowan, J.H., Jr., and Shaw, R.F. 2002. Recruitment. *In* Fishery science: the unique contributions of early life stages. *Edited by* L.A. Fuiman and R.G. Werner. Blackwell Science, Malden, Mass. pp. 88–111.

Cushing, D.H. 1990. Plankton production and year-class strength in fish populations: an update of the match/mismatch hypothesis. Adv. Mar. Biol. **26**: 249–293. doi:10.1016/S0065-2881(08)60202-3.

Deriso, R.B., Maunder, M.N., and Pearson, W.H. 2008. Incorporating covariates into fisheries stock assessment models with application to Pacific herring. Ecol. Appl. **18**(5): 1270–1286. doi:10.1890/07-0708.1. PMID:18686586.

Di Lorenzo, E., and Mantua, N. 2016. Multi-year persistence of the 2014/15 North Pacific marine heatwave. Nat. Clim. Change, **6**(11): 1042–1047. doi:10.1038/nclimate3082.

Dragesund, O., Østvedt, O.J., and Toresen, R. 2008. Norwegian spring-spawning herring: history of fisheries, biology and stock assessment. *In* Norwegian spring-spawning herring & northeast Arctic Cod: 100 years of research and management. *Edited by* O. Nakken. Tapir Academic, Trondheim, Norway. pp. 41–82.

Esri. 2020. World Countries (Generalized). ESRI. Redlands, Calif., USA. Available from https://hub.arcgis.com.

EVOSTC. 2010. Draft Integrated Herring Restoration Program July 21, 2010. EVOSTC, Anchorage, Alaska.

Flostrand, L.A., Schweigert, J.F., Daniel, K.S., and Cleary, J.S. 2009. Measuring and modelling Pacific herring spawning-site fidelity and dispersal using tag-recovery dispersal curves. ICES J. Mar. Sci. **66**(8): 1754–1761. doi:10.1093/icesjms/fsp151.

Funk, F.C., and Sandone, G.J. 1990. Catch-age analysis of Prince William Sound, Alaska, herring, 1973–1988. ADF&G Fish. Res. Bull. No. 90-01.

Gorman, K.B., Kline, T.C., Roberts, M.E., Sewall, F.F., Heintz, R.A., and Pegau, W.S. 2018. Spatial and temporal variation in winter condition of juvenile Pacific herring (*Clupea pallasii*) in Prince William Sound, Alaska: oceanographic exchange with the Gulf of Alaska. Deep-Sea Res. Part II Top. Stud. Oceanogr. **147**: 116–126. doi:10.1016/j.dsr2.2017.10.010.

Gray, B.P., Bishop, M.A., and Powers, S. 2019. Structure of winter groundfish feeding guilds in Pacific herring *Clupea pallasii* and walleye pollock *Gadus chalcogrammus* nursery fjords. J. Fish Biol. **95**: 527–539. doi:10.1111/jfb.13984.

Haegele, C.W., and Schweigert, J.F. 1985. Distribution and characteristics of herring spawning grounds and description of spawning behavior. Can. J. Fish. Aquat. Sci. **42**(S1): s39–s55. doi:10.1139/f85-261.

Haught, S., and Moffitt, S., 2018. ADFG Surveys: aerial survey route, biomass, age sex length, and spawn. Gulf of Alaska Data Portal. Available from https://portal.aoos.org [accessed 5 November 2018].

Hay, D.E. 1985. Reproductive biology of Pacific herring (*Clupea harengus pallasi*). Can. J. Fish. Aquat. Sci. **42**(S1): s111–s126. doi:10.1139/f85-267.

Hay, D.E., McCarter, P.B., and Daniel, K.S. 2001. Tagging of Pacific herring *Clupea pallasi* from 1936–1992: a review with comments on homing, geographic fidelity, and straying. Can. J. Fish. Aquat. Sci. **58**(7): 1356–1370 doi:10.1139/cjfas-58-7-1356, 10.1139/f01-087.

Hay, D.E., McCarter, P.B., and Daniel, K.S. 2008. Potential impacts of the British Columbia herring roe fishery on the spatial and temporal distribution of herring spawn: examination of the serial depletion hypothesis. Canadian Stock Assessment Secretariat, Nanaimo, B.C., Canada.

Hay, D.E., McCarter, P.B., Daniel, K.S., and Schweigert, J.F. 2009. Spatial diversity of Pacific herring (*Clupea pallasi*) spawning areas. ICES J. Mar. Sci. **66**(8): 1662–1666. doi:10.1093/icesjms/fsp139.

Hebert, K. 2019. Southeast Alaska 2018 Herring Stock Assessment Surveys. ADF&G, Fishery Data Series No. 19-12, Anchorage, Alaska.

Hershberger, P.K., Kocan, R.M., Elder, N.E., Meyers, T.R., and Winton, J.R. 1999. Epizootiology of viral hemorrhagic septicemia virus in Pacific herring from the spawn-on-kelp fishery in Prince William Sound, Alaska, USA. Dis. Aquat. Organ. **37**(1): 23–31. doi:10.3354/dao037023.

Holmes, E.E. 2013. Derivation of an EM algorithm for constrained and unconstrained multivariate autoregressive state-space (MARSS) models. arXiv:1302.3919 [stat.ME] Available from http://arxiv.org/abs/1302.3919 [accessed 6 November 2019].

Holmes, E., Ward, E., Scheuerell, M., and Wills, K. 2018*a* MARSS: Multivariate Autoregressive State-Space Modeling. Available from https://CRAN.R-project.org/package=MARSS.

Holmes, E.E., Ward, E.J., and Scheuerell, M.D. 2018*b*. Analysis of multivariate time-series using the MARSS package. Version 3.10.10. NOAA, National Marine Fisheries Service, Northwest Fisheries Science Center, 2725 Montlake Blvd. E., Seattle, WA 98112, USA [accessed 7 August 2019].

Holmes, E.E., Ward, E.J., and Wills, K. 2012. MARSS: Multivariate autoregressive state-space models for analyzing time-series data. R J. **4**(1): 11–19. doi:10.32614/RJ-2012-002.

Houde, E.D. 2016. Recruitment variability. In Fish reproductive biology. 2nd ed. *Edited by* T. Jakobsen, M.J. Fogarty, B.A. Megrey, and E. Moksness. Wiley-Blackwell, Oxford, UK. pp. 98–187.

Hulson, P.-J.F., Miller, S.E., Quinn, T.J., Marty, G.D., Moffitt, S.D., and Funk, F. 2008. Data conflicts in fishery models: incorporating hydroacoustic data into the Prince William Sound Pacific herring assessment model. ICES J. Mar. Sci. **65**(1): 25–43. doi:10.1093/icesjms/fsm162.

Huse, G., Fernö, A., and Holst, J.C. 2010. Establishment of new wintering areas in herring co-occurs with peaks in the 'first time/repeat spawner' ratio. Mar. Ecol. Prog. Ser. **409**: 189–198. doi:10.3354/meps08620.

Huse, G., Railsback, S., and Feronö, A. 2002. Modelling changes in migration pattern of herring: collective behaviour and numerical domination. J. Fish Biol. **60**(3): 571–582. doi:10.1111/j.1095-8649.2002.tb01685.x.

Incardona, J.P., Carls, M.G., Holland, L., Linbo, T.L., Baldwin, D.H., Myers, M.S., et al. 2015. Very low embryonic crude oil exposures cause lasting cardiac defects in salmon and herring. Sci. Rep. **5**: 13499. doi:10.1038/srep13499. PMID:26345607.

Keeling, B., Hessing-Lewis, M., Housty, C., Okamoto, D.K., Gregr, E.J., and Salomon, A.K. 2017. Factors driving spatial variation in egg survival of an ecologically and culturally important forage fish. Aquat. Conserv. Mar. Freshw. Ecosyst. **27**(4): 814–827. doi:10.1002/aqc.2757.

Lambert, T.C. 1987. Duration and intensity of spawning in herring *Clupea harengus* as related to the age structure of the mature population. Mar. Ecol. Prog. Ser. **39**(3): 209–220. doi:10.3354/meps039209.

Lambert, T.C. 1990. The effect of population structure on recruitment in herring. ICES J. Mar. Sci. **47**(2): 249–255. doi:10.1093/icesjms/47.2.249.

Ljungström, G., Francis, T.B., Mangel, M., and Jørgensen, C. 2019. Parent–offspring conflict over reproductive timing: ecological dynamics far away and at other times may explain spawning variability in Pacific herring. ICES J. Mar. Sci. **76**(2): 559–572. doi:10.1093/icesjms/fsy106.

MacCall, A.D., Francis, T.B., Punt, A.E., Siple, M.C., Armitage, D.R., Cleary, J.S., et al. 2019. A heuristic model of socially learned migration behaviour exhibits distinctive spatial and reproductive dynamics. ICES J. Mar. Sci. **76**(2): 598–608. doi:10.1093/icesjms/fsy091.

Macdonald, J.I., Logemann, K., Krainski, E.T., Sigurðsson, Þ., Beale, C.M., Huse, G., et al. 2018. Can collective memories shape fish distributions? A test, linking space-time occurrence models and population demographics. Ecography, **41**(6): 938–957. doi:10.1111/ecog.03098.

Marty, G.D., Quinn, T.J., II., Carpenter, G., Meyers, T.R., and Willits, N.H. 2003. Role of disease in abundance of a Pacific herring (*Clupea pallasi*) population. Can. J. Fish. Aquat. Sci. **60**(10): 1258–1265. doi:10.1139/f03-109.

Marty, G.D., Hulson, P.J.F., Miller, S.E., Tj Quinn, I.I., Moffitt, S.D., and Merizon, R.A. 2010. Failure of population recovery in relation to disease in Pacific herring. Dis. Aquat. Org. **90**(1): 1–14. doi:10.3354/dao02210.

McQuinn, I.H. 1997. Metapopulations and the Atlantic herring. Rev. Fish Biol. Fish. **7**(3): 297–329. doi:10.1023/A:1018491828875.

Moran, J.R., Heintz, R.A., Straley, J.M., and Vollenweider, J.J. 2018. Regional variation in the intensity of humpback whale predation on Pacific herring in the Gulf of Alaska. Deep-Sea Res. Part II, **147**: 187–195. doi:10.1016/j.dsr2.2017.07.010.

Morstad, S.P., Baker, T.T., and Brady, J.A. 1992. Pacific herring pound spawn-on-kelp fishery in Prince William Sound, Alaska, 1990. ADF&G, Regional Information Report 2A92-02, Anchorage, Alaska.

Muradian, M.L., Branch, T.A., Moffitt, S.D., and Hulson, P.-J.F. 2017. Bayesian stock assessment of Pacific herring in Prince William Sound, Alaska. PLoS ONE, **12**(2): e0172153. doi:10.1371/journal.pone.0172153. PMID:28222151.

Norcross, B., and Brown, E. 2001. Estimation of first-year survival of Pacific herring from a review of recent stage-specific studies. *In* Herring: Expectations for a new millennium. Alaska Sea Grant College Program, Fairbanks, Alaska, USA. pp. 535–558.

Okamoto, D.K., Hessing-Lewis, M., Samhouri, J.F., and Shelton, A.O. 2020. Spatial variation in exploited metapopulations obscures risk of collapse. Ecol. Appl. **15**: e02051. doi:10.1002/eap.2051.

Payne, L.X., Schindler, D.E., Parrish, J.K., and Temple, S.A. 2005. Quantifying spatial pattern with evenness indices. Ecol. Appl. **15**(2): 507–520. doi:10.1890/03-5029.

Pearson, W.H., Deriso, R.B., Elston, R.A., Hook, S.E., Parker, K.R., and Anderson, J.W. 2012. Hypotheses concerning the decline and poor recovery of Pacific herring in Prince William Sound, Alaska. Rev. Fish Biol. Fish, **22**(1): 95–135. doi:10.1007/s11160-011-9225-7.

Pearson, W.H., Elston, R.A., Bienert, R.W., Drum, A.S., and Antrim, L.D. 1999. Why did the Prince William Sound, Alaska, Pacific herring (*Clupea pallasi*) fisheries collapse in 1993 and 1994? Review of hypotheses. Can. J. Fish. Aquat. Sci. **56**(4): 711–737. doi:10.1139/f98-207.

Pegau, W.S. 2013. Community involvement, outreach, logistics, and synthesis. EVOS Prince William Sound Herring Survey Final Report, Prince William Sound Science Center, Cordova, Alaska.

Petitgas, P., Reid, D., Planque, B., Nogueira, E., O'Hea, B., and Cotano, U. 2006. The entrainment hypothesis: an explanation for the persistence and innovation in spawning migrations and life cycle spatial patterns. ICES CM 2006/B:07. Available from http://www.ices.dk/sites/pub/CM%20Doccuments/2006/B/B0706.pdf [accessed 23 May 2020].

Pielou, E.C. 1966. The measurement of diversity in different types of biological collections. J. Theor. Biol. **13**: 131–144. doi:10.1016/0022-5193(66)90013-0.

Pineda, J., Hare, J.A., and Sponaugle, S. 2007. Larval transport and dispersal in the coastal ocean and consequences for population connectivity. Oceanog. **20**(3): 22–39. doi:10.5670/oceanog.2007.27.

Quinn, T.J., Marty, G.D., Wilcock, J., and Willette, M. 2001. Disease and population assessment of Pacific herring in Prince William Sound, Alaska. *In* Herring: expectations for a new millennium. *Edited by* F. Funk, J. Blackburn, D. Hay, A.J. Paul, and R. Stephanson. University of Alaska Sea Grant, Anchorage, Alaska. pp. 363–379.

R Core Team. 2020. R: a language and environment for statistical computing. R Foundation for Statistical Computing, Vienna, Austria. Available from http://www.R-project.org/.

Rice, S.D., and Carls, M.G. 2007. Prince William Sound herring: an updated synthesis of population declines and lack of recovery. Restoration Project 050794. Final Report. NOAA, National Marine Fisheries Service, Alaska Fisheries Science Center, Auke Bay Laboratories, Juneau, Alaska.

Rice, S.D., Moran, J.R., Straley, J.M., Boswell, K.M., and Heintz, R.A. 2011. Significance of whale predation on natural mortality rate of Pacific herring in Prince William Sound. Final Report. NOAA, National Marine Fisheries Service, Alaska Fisheries Science Center, Auke Bay Laboratories, Juneau, Alaska.

Rogers, L.A., and Dougherty, A.B. 2019. Effects of climate and demography on reproductive phenology of a harvested marine fish population. Global Change Biol. **25**(2): 708–720. doi:10.1111/gcb.14483.

Rooper, C.N., Haldorson, L.J., and Quinn, T.J., II. 1999. Habitat factors controlling Pacific herring (*Clupea pallasi*) egg loss in Prince William Sound, Alaska. Can. J. Fish. Aquat. Sci. **56**(6): 1133–1142. doi:10.1139/f99-050.

Russell, C.W., Botz, J., Haught, S., and Moffitt, S. 2017. 2016 Prince William Sound Area Finfish Management Report. ADF&G, Fishery Management Report 17-37, Anchorage, Alaska.

Ruzzante, D.E., Mariani, S., Bekkevold, D., André, C., Mosegaard, H., Clausen, L.A.W., et al. 2006. Biocomplexity in a highly migratory pelagic marine fish, Atlantic herring. Proc. R Soc. B Biol. Sci. **273**(1593): 1459–1464. doi:10.1098/rspb.2005.3463. PMID:16777738.

Schindler, D.E., Hilborn, R., Chasco, B., Boatright, C.P., Quinn, T.P., Rogers, L.A., and Webster, M.S. 2010. Population diversity and the portfolio effect in an exploited species. Nature, **465**(7298): 609–612. doi:10.1038/nature09060. PMID:20520713.

Shannon, C.E., and Weaver, W. 1949. The mathematical theory of communication. University of Illinois Press, Urbana, Ill., USA.

Shelton, A.O., Francis, T.B., Williams, G.D., Feist, B., Stick, K., and Levin, P.S. 2014. Habitat limitation and spatial variation in Pacific herring egg survival. Mar. Ecol. Prog. Ser. **514**: 231–245. doi:10.3354/meps10941.

Shepherd, C.S., and Haught, S. 2019. Pacific herring aerial surveys and age, sex, and size processing in the Prince William Sound Area, 2018–2021. ADF&G, Regional Operational Plan ROP.CF.2A.2019.05, Cordova, Alaska.

Sinclair, M., and Tremblay, M.J. 1984. Timing of spawning of Atlantic herring (*Clupea harengus harengus*) populations and the match–mismatch theory. Can. J. Fish. Aquat. Sci. **41**(7): 1055–1065. doi:10.1139/f84-123.

Siple, M.C., and Francis, T.B. 2016. Population diversity in Pacific herring of the Puget Sound, USA. Oecologia, **180**(1): 111–125. doi:10.1007/s00442-015-3439-7. PMID:26427990.

Thorne, R.E., and Thomas, G.L. 2008. Herring and the “Exxon Valdez” oil spill: an investigation into historical data conflicts. ICES J. Mar. Sci. **65**(1): 44–50. doi:10.1093/icesjms/fsm176.

Ward, E.J., Adkison, M., Couture, J., Dressel, S.C., Litzow, M.A., Moffitt, S., et al. 2017. Evaluating signals of oil spill impacts, climate, and species interactions in Pacific herring and Pacific salmon populations in Prince William Sound and Copper River, Alaska. PLoS ONE, **12**(3): e0172898. doi:10.1371/journal.pone.0172898. PMID:28296895.

Ward, E.J., Chirakkal, H., González-Suárez, M., Aurioles-Gamboa, D., Holmes, E.E., and Gerber, L. 2010. Inferring spatial structure from time-series data: using multivariate state-space models to detect metapopulation structure of California sea lions in the Gulf of California, Mexico. J. Appl. Ecol. **47**(1): 47–56. doi:10.1111/j.1365-2664.2009.01745.x.

Ware, D., and Schweigert, J. 2001. Metapopulation structure and dynamics of British Columbia herring. Fisheries and Oceans Canada, Canadian Science Advisory Secretariat, Nanaimo, B.C., Canada.

Ware, D.M., and Tanasichuk, R.W. 1989. Biological basis of maturation and spawning waves in Pacific herring (*Clupea harengus pallasi*). Can. J. Fish. Aquat. Sci. **46**(10): 1776–1784. doi:10.1139/f89-225.

Ware, D.M., Tovey, C., Hay, D., and McCarter, B. 2000. Straying rates and stock structure of British Columbia herring. Fisheries and Oceans Canada, Canadian Science Advisory Secretariat, Nanaimo, B.C., Canada.

Wildes, S.L., Nguyen, H., and Guyon, J.R. 2018. Genetic stock structure of herring in Prince William Sound. *Exxon Valdez* Long-Term Herring Research and Monitoring Program Final Report, EVOSTC, Anchorage, Alaska.